Progress in Oceanography 87 (2010) 127–143

Contents lists available at ScienceDirect

Progress in Oceanography

journal homepage: www.elsevier.com/locate/pocean

Changes in the freshwater composition of the upper ocean west of the Antarctic Peninsula during the first decade of the 21st century

Michael P. Meredith [a,*], Margaret I. Wallace [a,1], Sharon E. Stammerjohn [b], Ian A. Renfrew [c], Andrew Clarke [a], Hugh J. Venables [a], Deborah R. Shoosmith [a], Terri Souster [a], Melanie J. Leng [d]

[a] British Antarctic Survey, High Cross, Madingley Road, Cambridge, United Kingdom
[b] Ocean Sciences Department, University of California, Santa Cruz, CA, United States
[c] School of Environmental Sciences, University of East Anglia, Norwich, United Kingdom
[d] NERC Isotope Geosciences Laboratory, British Geological Survey, Keyworth, United Kingdom

A B S T R A C T

In recent decades, the west Antarctic Peninsula (WAP) has warmed more rapidly than anywhere else in the Southern Hemisphere. Associated with this, there has been a marked shortening of the sea ice season, a retreat of the majority of glaciers, and an increase in precipitation. Each of these changes in the freshwater system has the potential to exert significant influence on the ecosystem, via processes such as stabilisation of the upper water column, and supply of micronutrients to the mixed layer. Here we use a time series of hydrographic and stable oxygen isotope ($\delta^{18}O$) measurements collected at a near-coastal site in Marguerite Bay to quantify the prevalence of meteoric freshwater (glacial melt plus precipitation) separately from sea ice melt. During 2002–2009, meteoric water dominated, with summer water column inventories of order 4–6 m. Summer sea ice melt inventories were lower, ranging from −1 to 0.5 m (where a negative value indicates net sea ice formation from this water). In the near-surface layers, we find highest meteoric water prevalence in February 2006 (~6%) and lowest in October 2007 (~1%), whilst sea ice melt is highest in February 2005 (2%) and lowest in July 2002 (−2%). The ranges in both meteoric water and sea ice melt are significantly larger than derived previously using a subset of the data, reflecting the strong interannual variability present. The largest single determinant of the near-surface freshwater percentages is found to be changes in mixed layer depth. Notably deep layers occurred in the winters of 2003, 2007 and 2008, due to northerly winds associated with El Niño/Southern Oscillation and the Southern Annular Mode. These led to greatly reduced sea ice cover in northern Marguerite Bay, and allowed persistent air-sea heat fluxes and stronger rates of sea ice production, which is a key factor in controlling mixed layer depth. We also discuss the possible role of interannual changes in wind-induced mixing in this context. As climate change at the WAP continues, we expect further changes in each of the components of the freshwater budget, and also changes in the vertical redistribution of this freshwater by oceanographic processes. Our ongoing $\delta^{18}O$ monitoring will help track these changes, and elucidate their consequences for the operation of the marine ecosystem.

1. Introduction

The region west of the Antarctic Peninsula (Fig. 1) is one of the most rapidly warming in the world (King, 1994; Vaughan et al., 2003). Atmospheric temperatures here rose during the second half of the twentieth century at a rate exceeding that of any other region in the Southern Hemisphere, and paralleled by only two areas in the Northern Hemisphere (northwestern North America and the Siberian Plateau (Trenberth et al., 2007)). Because the west Antarctic Peninsula (WAP) is the only one of these three regions to have a maritime climate, it is the best place in the world to study the drivers, feedbacks and ecological consequences of rapid climate change as they relate to an oceanic environment (Schofield et al., 2010).

Annual mean warming based on Antarctic Peninsula station data was 3.7 ± 1.6 °C/century unweighted, or 3.4 °C/century when weighted by length of record (Vaughan et al., 2003). The warming is concentrated most strongly in the austral autumn and winter (King and Harangozo, 1998; Turner et al., 2005), and whilst the last generation of IPCC-class coupled climate models was able to reproduce a warming at the Peninsula that was qualitatively consistent with that observed (Bracegirdle et al., 2008), the underlying mechanisms for the warming, and its strong seasonality, have not yet been fully determined. Notwithstanding this, there is evidence that

* Corresponding author. Tel.: +44 1223 221586; fax: +44 1223 221226.
E-mail address: mmm@bas.ac.uk (M.P. Meredith).
[1] Present address: British Oceanographic Data Centre, Joseph Proudman Building, Brownlow Street, Liverpool, United Kingdom.

0079-6611/$ - see front matter © 2010 Elsevier Ltd. All rights reserved.
doi:10.1016/j.pocean.2010.09.019

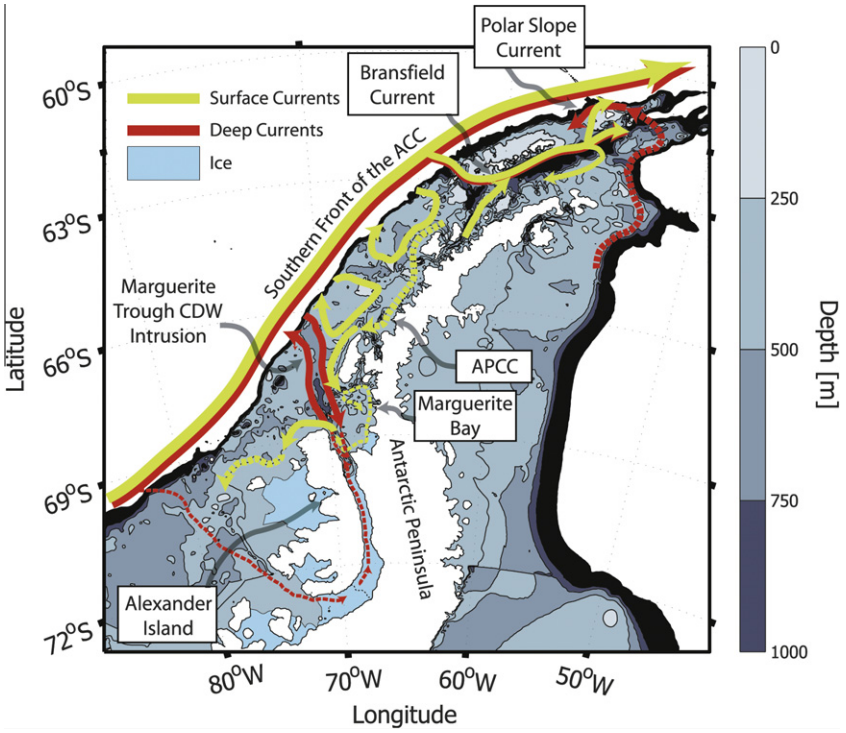

Fig. 1. Schematic of the circulation at the western Antarctic Peninsula, divided into surface circulation pattern (green) and deep circulation pattern (red). Dotted lines are tentative flows. Figure courtesy of C. Moffat and R. Beardsley (WHOI), following Beardsley et al. (2007).

temperatures at the WAP are strongly correlated with patterns of atmospheric circulation, whereby anomalously warm winters at the WAP are associated with more cyclonic conditions and increased warm-air advection (Turner et al., 1997). Following this pattern, the trend to higher temperatures at the WAP could well have been accompanied by a shift to more cyclonic circulation in the atmosphere, consistent with evidence for increased precipitation at the WAP in recent decades (Thomas et al., 2008). It was shown recently that the significant warming over the last half century was prevalent throughout all of West Antarctica, and not constrained just to the Peninsula (Steig et al., 2009). Shallow ice core evidence has confirmed this, and has also shown that the regional warming began around 1900, and that the temperature trend is likely the result of external climate forcing (Thomas et al., 2009).

The role of the ocean in WAP climate change is still being investigated. It is clear that the deep waters of the Antarctic Circumpolar Current (ACC), which lies adjacent to the WAP, have warmed strongly in recent decades (Gille, 2008). This water, termed Circumpolar Deep Water (CDW), penetrates the WAP shelf, becoming modified via interaction with overlying water masses as it does so (Hofmann et al., 1996; Klinck, 1998; Smith et al., 1999). It intrudes on the shelf most readily via the deep glacially-scoured troughs that cut across it, and provides a source of heat, salt and nutrients to the WAP shelf (Klinck, 1998; Smith et al., 1999). It has been shown from both models and observations that the strengthening of the circumpolar winds over the Southern Ocean can act to promote CDW intrusion onto the shelf regions of west Antarctica, including the WAP (Martinson et al., 2008; Thoma et al., 2008).

The role of upper ocean processes in WAP climate change has also been investigated, and it has been shown that summer temperatures of the near-surface ocean rose here during the second half of the twentieth century by well over 1 °C, and that there was a concordant strong salinification of the upper ocean (Meredith and King, 2005). It was argued that these changes were induced by the trends in the atmospheric circulation and temperature, and also by related changes in the sea ice field (see below), but that they acted as positive feedbacks to enhance and sustain the atmospheric warming. It is also worth noting that the role of the upper ocean (storing heat in the summer and releasing it back to the atmosphere in winter) will shift the seasonal phase of any long-term atmospheric trend, and hence could explain at least some of the marked seasonality in the WAP atmospheric warming.

In addition to its influence on precipitation, the climatic change at the WAP has exerted a marked influence on the other components of the freshwater system. Of particular note is a trend toward decreased winter sea ice duration at the WAP (Smith and Stammerjohn, 2001; Vaughan et al., 2003; Stammerjohn et al., 2008b), contrasting with weaker sea ice trends elsewhere in the Southern Ocean and a strong positive trend in the western Ross Sea (Stammerjohn et al., 2008b; Turner et al., 2009). The decrease in sea ice season at the WAP is caused primarily by a strong trend toward a later advance in autumn, and a weaker trend toward an earlier retreat in spring (Stammerjohn et al., 2008b).

The climatic change at the WAP has also had a profound effect on the glacial ice field. It was shown that more than 80% of the glaciers at the Peninsula retreated during the second half of the twentieth century, and that average retreat rates have been accelerating (Cook et al., 2005). Further, the rise in atmospheric temperature at the WAP has led to an increase in the annual duration of melt conditions here, and whilst the majority of the meltwater will refreeze within the ice sheet, there are nonetheless signs that an increase in runoff will occur (Vaughan, 2006).

In an ecosystem context, it is important to understand the changes in the freshwater budget of the WAP on a range of timescales, including seasonal, interannual and decadal. One reason for this is that freshwater input to the surface ocean has a strong stabilising influence, as a consequence of salinity being the dominant term in the equation of state for seawater at low temperature. Consequently, a thin layer of sea ice melt supplied to the ocean in spring has the potential to greatly stabilise the ocean and create

conditions that are more favourable for phytoplankton bloom development by retaining the biological cells in a favourable light environment (Mitchell and Holm-Hansen, 1991). A layer of glacial ice melt can act in the same way (Dierssen et al., 2002), and also has the potential to supply micronutrients such as iron to the surface ocean, resulting from the scouring of underlying rock and sediment and the accumulation from atmospheric deposition. Indeed, it has been contended that continued warming at the WAP and an increase in runoff from glaciers could lead to a shift in phytoplankton assemblage composition and an increase in biomass in coastal waters (Dierssen et al., 2002).

Recently, it was shown that the transition from a polar to subpolar climate that the WAP is undergoing has had a profound impact on productivity, with phytoplankton biomass decreasing between the late 1970s/early 1980s and the last decade (Montes-Hugo et al., 2009). This change comprised separate trends in the northern and southern WAP regions, with phytoplankton biomass decreasing in the north due to increased cloudiness and winds (and hence greater wind-driven mixing), but increasing in the south due to decreasing sea ice and clouds combined with greater water column stratification. It was noted that these regional changes had consequences for higher trophic levels, including Antarctic krill and penguin populations (Montes-Hugo et al., 2009). The role of sea ice in controlling upper-ocean stratification and freshwater input in the southern WAP region is thus one of the key factors in influencing the ecosystem.

Whilst measurements of salinity are, in theory, sufficient to quantify changes in the overall freshwater input to the WAP ocean, they do not by themselves provide understanding of the causes of such changes. However, this understanding is needed if a level of predictive skill is to be generated, and the future freshwater impacts on the marine ecosystem determined. In this context, measurements of the stable isotopes of oxygen ($\delta^{18}O$, the standardised ratio of $H_2{}^{18}O$ to $H_2{}^{16}O$ in seawater) are extremely useful, since they enable quantification of sea ice melt input to the ocean separately from freshwater input from other sources (Craig and Gordon, 1965). In a previous paper (Meredith et al., 2008a), we used two years of $\delta^{18}O$ data (2002 and 2003) from a near-coastal site at the WAP to investigate the seasonal changes in the constituents of the freshwater balance. It was found that meteoric water (mostly in the form of glacial melt) was the dominant freshwater source, accounting for up to 5% of the near-surface ocean during summer. Sea ice melt was much less significant, even during summer (maximum prevalence was around 1%), and it was found that the seasonality in the glacial melt and sea ice melt signals was similar (around 1–2%).

A much longer series of $\delta^{18}O$ is now available at the WAP, specifically covering 2002–2009. Invoking the rule of thumb that a time series is worth revisiting each time it has at least doubled in length (e.g. Stammer et al., 2006), we here use this longer series to address questions relating to the interannual variability of the freshwater balance of the WAP during the first decade of the 21st century, the representativeness of the data over a wider area, and the causes of the changes observed.

2. Background and context

2.1. Circulation and water masses at the WAP

The ocean circulation at the WAP is shown schematically in Fig. 1, with surface and deeper patterns of flow illustrated separately. The upper layer circulation consists of a strong surface circulation adjacent to the shelf slope, associated with the eastward flow of the southernmost front of the ACC. This flow can intrude onto the shelf in places, most notably toward the northern end of the western Peninsula, and can also form the outermost edge of semi-closed gyre-like circulations over the shelf (Klinck et al., 2004). Closer to the continent, a coastal current flows southward along the western side of Adelaide Island, and also along the northern and western sides of Alexander Island (Stein, 1992; Moffat et al., 2008; Savidge and Amft, 2009). This current, dubbed the Antarctic Peninsula Coastal Current (APCC), is a narrow feature that exhibits some seasonal variability, and is believed to be at least partially buoyancy-forced by freshwater supply from coastal runoff. Between Adelaide Island and Alexander Island lies Marguerite Bay, which is the primary focus of the present study (Fig. 2). The pathway of the APCC within Marguerite Bay is not well constrained by available data, though cyclonic flow within the bay has been evidenced by drifters and other means (Beardsley et al., 2004; Savidge and Amft, 2009).

The upper layer circulation at the WAP comprises Antarctic Surface Water (AASW), which in winter consists of a homogeneous layer of water around 50–100 m thick, with temperatures close to the freezing point and salinities around 33.5–34.0. During spring and summer, the melt of sea ice and glacial ice freshens the very surface layer, which is also heated via insolation. This leads to a warmer, fresher cap undercut by the cold remnant of the winter mixed layer, which is now characterised by a minimum in potential temperature and termed Winter Water (WW; Mosby, 1934).

The AASW layer is separated by a pycnocline from the deeper circulation below. This deeper circulation is dominated by the inflow of CDW from the ACC onto the shelf, which occurs preferentially in regions where deep troughs cut across the shelf (e.g. Klinck et al., 2004; Martinson et al., 2008). Momentum advection and curvature of the shelf break is believed to be important in driving this CDW onto the shelf (Dinniman and Klinck, 2004). In the context of the present work, the Marguerite Trough is especially important, since it runs south and east from the shelf break into Marguerite Bay, providing a deep conduit for CDW into this locality. Maximum depths of Marguerite Trough are around 1600 m, close to Alexander Island (Fig. 2).

CDW is a warm, saline water mass by comparison with other waters on the WAP shelf, having potential temperatures >1.0 °C and salinities in the range 34.60–34.74, and is also characterised by high levels of macronutrients. Because of the ecological impact of the heat and nutrients delivered to the shelf by CDW, there has been marked interest in the frequency of its intrusions. It has been argued that four to six inflow events typically occur in a year (Klinck et al., 2004), while more recent studies have highlighted the importance of variability in inflow on timescales characteristic of eddy processes (Moffat et al., 2009).

For CDW to have a particular impact on the upper-ocean ecosystem at the WAP, there must be significant vertical exchange for it to supply heat and nutrients to the mixed layer (Martinson, 1990). Various mechanisms exist that will facilitate this, including seasonal deepening of the mixed layer and excavation of the underlying CDW (Meredith et al., 2004), diffusive-convective instability (Smith and Klinck, 2002), internal tides, and wind-induced coastal upwelling and downwelling (Wallace et al., 2008). The spatial pattern and magnitudes of these processes is the subject of ongoing investigations.

2.2. Coupled modes of climate variability and the WAP

Insight into the causes of the interannual signals in our multi-year $\delta^{18}O$ series requires an understanding of the forcing mechanisms that can generate variability at the WAP on these timescales. There are two such mechanisms that have received much attention in recent years, specifically the El Niño/Southern Oscillation (ENSO) phenomenon (Turner, 2004), and the Southern Annular Mode (SAM; Thompson and Solomon, 2002). The spatial impact

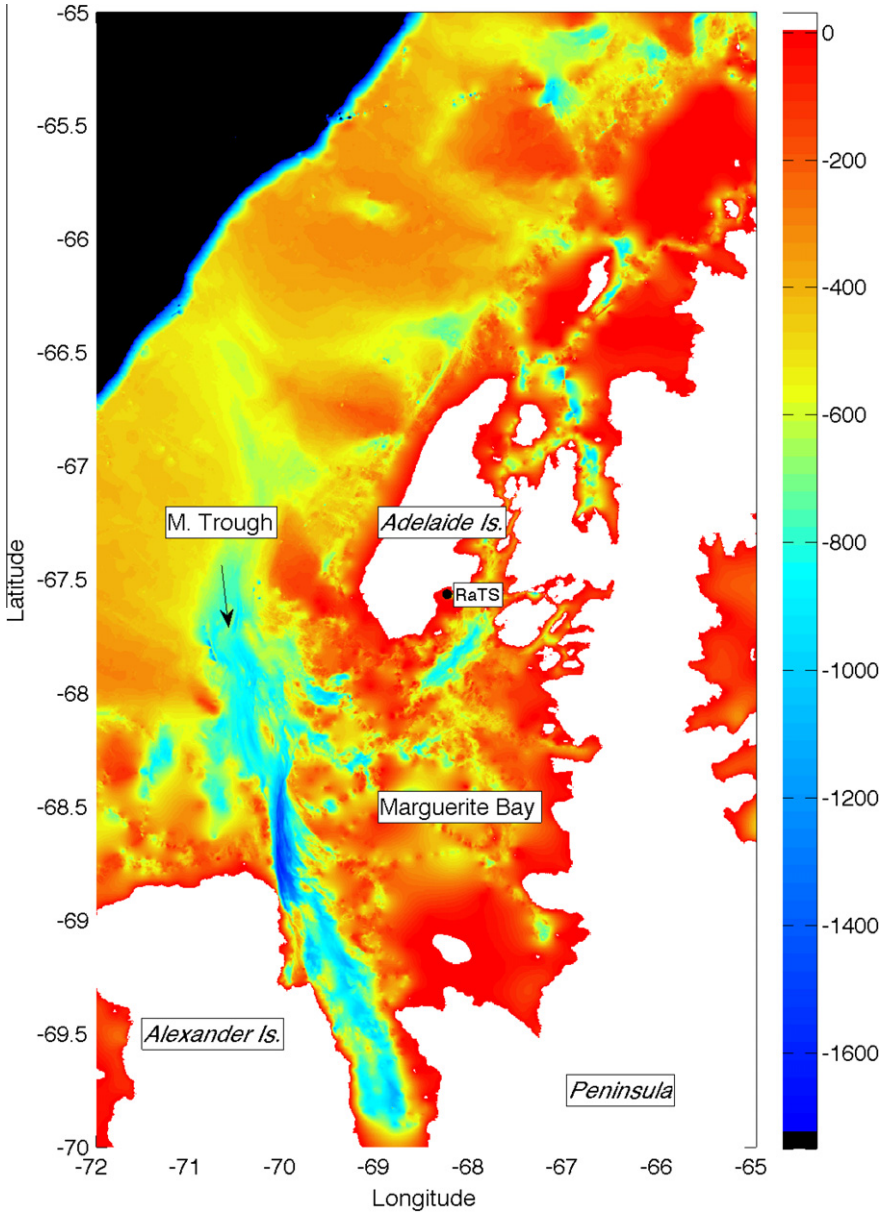

Fig. 2. Detailed bathymetry of Marguerite Bay and the immediate vicinity, from the Southern Ocean GLOBEC bathymetric dataset. The RaTS site, immediately adjacent to Rothera Station on Adelaide Island, is marked.

of these modes on the surface atmospheric pressure field is shown in Fig. 3.

The first of these modes, ENSO, is the characteristic switching of the surface pressure anomaly between the Indian Ocean–Australian region and the southeastern tropical Pacific. ENSO signals can propagate to high latitudes via an atmospheric Rossby wave train, with particular impact in the southeast Pacific and the region of the WAP (Fig. 3; see also Turner (2004)). The contrasting atmosphere–ocean-ice responses east and west of the high latitude pressure anomaly (Fig. 3), and the possible mechanistic linkages involved, were described by Yuan (2004). A previous investigation of hydrographic data from northern Marguerite Bay noted a very deep mixed layer during the winter of 1998, and ascribed this to the effects of the very strong El Niño event that was then decaying (though the positive SAM condition, especially during April–August, is now seen to be potentially also a key factor). The specific mechanism to explain the deep mixed layer was anomalous northerly winds advecting sea ice away from the northern edge of Marguerite Bay, thereby maintaining open water and leading to enhanced ice production and densification of the upper ocean (Meredith et al., 2004). It is important to note, however, that individual El Niño events can be different (including in the nature and extent of their modification by SAM (Fogt and Bromwich, 2006)), and it cannot be assumed that they will all have the same atmospheric signal at the WAP, nor the same ocean response (Turner, 2004).

The second of these modes, the SAM, is the dominant mode of extratropical atmospheric circulation in the Southern Hemisphere (Thompson and Solomon, 2002). The SAM has a much more zonally-symmetric structure than ENSO, and comprises (to a first-order approximation) a node over Antarctica and an annulus over the lower latitudes of the Southern Ocean (Fig. 3). Atmospheric mass is exchanged between these centers of action on timescales from weeks to decades (Thompson and Wallace, 2000; Thompson et al., 2000; Marshall, 2003), with corresponding changes in the strength of the circumpolar winds overlying the Southern Ocean.

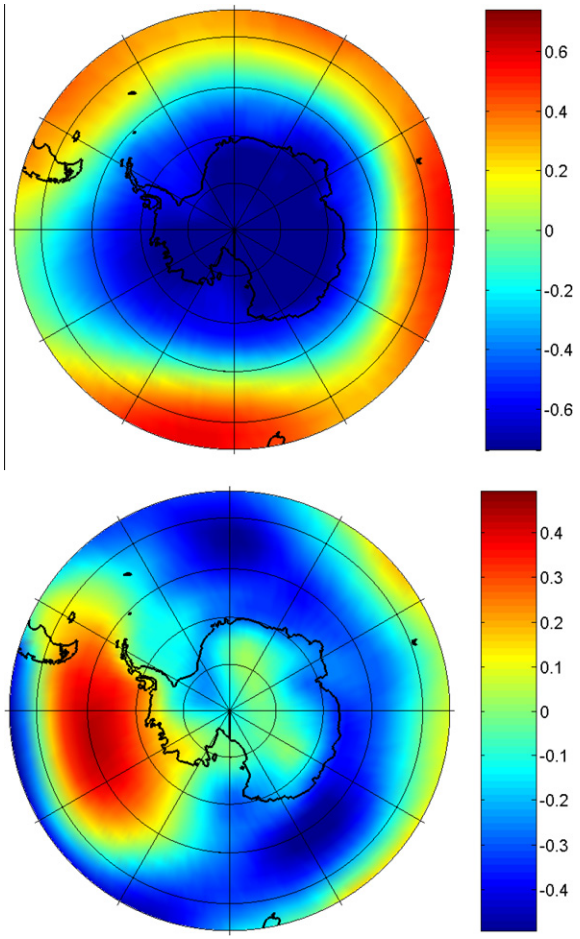

Fig. 3. One-point correlation maps of (top) SAM and bottom (ENSO) time series with surface atmospheric pressure over Antarctica and the Southern Ocean. Note the strong footprint of ENSO in the Southeast Pacific and at the WAP. SAM has a more zonally-symmetric structure, but with its most non-zonal component occurring in the south Pacifc and at the WAP.

The SAM pattern is not completely zonally-symmetric, however, and has its largest asymmetry in the southern Pacific; here it can induce significant anomalies in meridional winds on the timescales at which it operates. In turn, the contrasting meridional winds east and west of this asymmetric pressure anomaly induce contrasting ice-edge anomalies (Lefebvre et al., 2004; Lefebvre and Goosse, 2005).

Given the juxtaposition of the SAM and ENSO spatial patterns seen in Fig. 3, several studies have examined their combined impacts on Antarctic climate (Kwok and Comiso, 2002; L'Heureux and Thompson, 2006; Liu et al., 2004; Stammerjohn et al., 2008b). Their impacts on sea surface temperatures across the Pacific sector of the Southern Ocean (including the WAP) and into the Atlantic were discussed by Meredith et al. (2008b), with specific focus on understanding the ocean/atmosphere feedbacks that sustain the propagating oceanic signals. Liu et al. (2004) showed that ENSO and SAM-related sea ice changes contributed to regionally opposing sea ice trends, with largest decreases in the Bellingshausen/eastern Amundsen Seas, versus increases in the western Ross Sea. Seasonally, the largest changes in both regions are during spring sea ice retreat and autumn sea ice advance. This is also consistent with the seasonal atmospheric changes associated with ENSO and SAM: beginning in the 1990s, the high latitude atmospheric response intensified during austral spring-summer (e.g. Fogt and Bromwich (2006)), and SAM became more positive during summer-autumn (Marshall, 2003; Turner et al., 2009). The latter is implicated in asymmetrically strengthening the high latitude response to La Niña over El Niño events, and together they help to explain the wind-driven sea ice decreases in the greater WAP region (Stammerjohn et al., 2008b).

3. Methods

3.1. Hydrographic data

The presence of the British Antarctic Survey research station at Rothera Point on Adelaide Island (Fig. 2) has enabled sustained, year-round observations to be made in northern Marguerite Bay since 1997. This monitoring programme, the Rothera Oceanographic and Biological Time Series (RaTS), includes measurement of a range of physical, biogeochemical and biological parameters (full details available at www.antarctica.ac.uk/rats). Of interest here are the quasi-weekly water column profiles collected with a Conductivity-Temperature-Depth (CTD) probe. Initially, the CTD unit used was a Chelsea Instruments Aquapack, but this was replaced in early 2003 with a SeaBird SBE19. During a standard RaTS event, the CTD is lowered and raised using a handcranked winch, with the instrument operated in internal-recording mode, and data downloaded at Rothera immediately after collection. Such profiling is conducted from rigid inflatable boat during the ice-free season, and through a hole cut in the sea ice during periods of sufficiently heavy ice cover in winter. Data precision is maintained by regular joint casts of the RaTS CTD with SeaBird 911*plus* CTD units carried by *RRS James Clark Ross* and *ARSV Laurence M. Gould,* with offsets applied to the RaTS salinity data to reconcile them with the SBE911*plus* data.

In addition to the quasi-weekly CTD profiling undertaken by RaTS and the annual CTD profiles obtained during relief of Rothera, we have also collected CTD data during a more extensive research cruise in northern Marguerite Bay (JR137/150). This was conducted in February 2006, with all casts conducted to within 10 m of the seabed using the SBE911*plus* CTD onboard *RRS James Clark Ross*.

3.2. Stable isotope sampling collection and analysis

During a standard RaTS event, discrete water samples are collected from the upper ocean using a Niskin bottle lowered to 15 m depth and closed with a brass messenger weight. For the present work, samples for $\delta^{18}O$ analysis were stored in 150-ml medical flat bottles, with rubber inserts in the caps. These were sealed further with Parafilm to prevent slippage of the cap, and hence eliminate evaporation. Samples were transported to the UK annually in batches via cool stow (4 °C) and in the dark. These were analysed at the Natural Environment Research Council Isotope Geosciences Laboratory (NIGL) at the British Geological Survey, Keyworth. The analysis procedure uses the equilibration method for oxygen, following Epstein and Mayeda (1953), and a VG Isoprep 18 and Sira 10 mass spectrometer. Random duplicates were run to assess data integrity; average precision better than ±0.02‰ was obtained.

During CTD casts conducted from *RRS James Clark Ross* close to the RaTS site, we have frequently taken the opportunity to obtain isotope samples from a range of depth levels using the rosette multisampler available, so as to better understand the vertical distribution of the freshwater composition of the WAP ocean. These samples were stored and transported in the same way as RaTS $\delta^{18}O$ samples. Similarly, CTD casts from the JR137/150 cruise in northern and western Marguerite Bay were sampled for $\delta^{18}O$ at various levels in the vertical, and samples handled identically.

3.3. Quantification of freshwater contributions using stable isotope data

The great utility of $\delta^{18}O$ as a tracer of freshwater in the polar oceans derives from its different behaviour to salinity. Meteoric water input to the ocean (from glacial melt or precipitation) has low salinity (normally zero or very close to zero). Sea ice melt has a slightly higher salinity, but measurements of the salinity of seawater are not sufficient to distinguish sea ice melt from meteoric water input. The use of $\delta^{18}O$ in addition to salinity has significant benefit in this context, since meteoric water at high latitudes is typically very isotopically light (low $\delta^{18}O$ values), whilst sea ice melt has a very similar $\delta^{18}O$ to the seawater from which it formed (Lehmann and Siegenthaler, 1991), and is hence significantly isotopically heavier. Consequently, measuring both tracers simultaneously enables freshwater of meteoric origin to be distinguished from sea ice melt. This has been used to great effect in a range of studies, including investigations of the input of glacial melt into the precursors of Antarctic Bottom Water (Weiss et al., 1979; Schlosser et al., 1990; Weppernig et al., 1996) and to determine the freshwater composition of upper-layer water masses in both polar regions (Bauch et al., 1995; Schlosser et al., 2002; Meredith et al., 2008a).

Since both salinity and $\delta^{18}O$ tracers are conservative in the ocean, they can be used to distinguish meteoric water from sea ice melt in a quantitative way, using a simple three-endmember mass balance (after Östlund and Hut (1984)):

$$\begin{aligned} f_{sim} + f_{met} + f_{cdw} &= 1 \\ S_{sim}f_{sim} + S_{met}f_{met} + S_{cdw}f_{cdw} &= S \\ \delta_{sim}f_{sim} + \delta_{met}f_{met} + \delta_{cdw}f_{cdw} &= \delta \end{aligned} \quad (1)$$

where f_{sim}, f_{met} and f_{cdw} are the fractions of sea ice melt, meteoric water and CDW to be derived. S_{sim}, S_{met}, S_{cdw}, δ_{sim}, δ_{met} and δ_{cdw} are the corresponding salinity and $\delta^{18}O$ endmember values (see below), of which the products with the respective freshwater fractions total the measured salinity (S) and measured $\delta^{18}O$ (δ) of each water sample. (Since there are as many constraining equations as unknowns, a solution is found that exactly reconciles the derived freshwater fractions with observed salinity and $\delta^{18}O$ values).

The choice of endmember values (the values of "pure" meteoric water and sea ice melt, and undiluted CDW) is detailed fully in Meredith et al. (2008a). In summary, the endmember for meteoric water is taken to have a salinity of zero, and a $\delta^{18}O$ value of $-17‰$, with the latter based on published values for precipitation and ice flux onto the WAP shelf (Potter and Paren, 1985). The salinity of sea ice melt is taken to be 7, which is a reasonable representative value for this region (Meredith et al., 2008a), and the corresponding $\delta^{18}O$ endmember is taken to be 2.1‰ (i.e. a realistic $\delta^{18}O$ value for surface waters, plus an offset for fractionation). The salinity endmember is set as 34.62, and the corresponding $\delta^{18}O$ value is -0.08‰; these are the typical values obtained from measurements at the deepest level at the RaTS site, and hence represent the modified form of CDW that intrudes into Marguerite Bay, and relative to which the observed freshening is here quantified. Typical errors in the derived freshwater percentages resulting from the uncertainty in choice of endmembers and measurement error are around ±1%. If vertical profiles of salinity and $\delta^{18}O$ are available, column integrals of meteoric water and sea ice melt can be derived by first calculating the profiles of f_{sim} and f_{met} (using Eq. (1)), and then integrating in the vertical.

3.4. Meteorological and sea ice observations

Direct observations of sea ice type and concentration have been made from Rothera throughout the period of RaTS, with ice type flagged as "brash", "pack", "grease", "pancake" or "fast". A weighting scheme is employed to convert these to an overall ice score. Within this scheme, brash and pack ice are given the lowest scores (0.1), since they largely blow in and out of the sampling region rather than forming and melting *in situ*. Grease and pancake ice have higher scores (0.5), since they form *in situ* but are generally quite thin, and do not contribute much to freshwater dynamics. Fast ice has the highest weighting (1), since it is the dominant ice type in controlling the processes in which we are interested. Using this scheme, a score of zero denotes ice-free conditions, and a score of 10 denotes complete fast ice cover. The interannual variability in the time series of ice score used here shows strong correspondence with year-on-year changes in sea ice concentration measured further north on the WAP shelf (e.g. Fig. 8 of Ducklow et al. (2010)), testifying to the large-scale representativeness of the data.

Meteorological measurements made from Rothera include mean sea level pressure, 10 m winds, 2 m air temperature, 2 m relative humidity, and cloud fraction; these are available at 3-hourly intervals. These measurements were used to construct a surface energy budget for the RaTS site, where the total heat flux from the ocean to the atmosphere (Q_{tot}) is derived as:

$$Q_{tot} = Q_s + Q_l + Q_r \quad (2)$$

where Q_s, Q_l and Q_r are the sensible, latent and net radiative heat fluxes respectively. The derivation of the turbulent heat fluxes over open water at the freezing point follows a stability-dependent algorithm based on Smith (1988) and DeCosmo et al. (1996). The long- and short-wave radiative fluxes are calculated from sea surface temperature, air temperature, cloud cover and humidity, using empirical formulae. These can be surprisingly accurate for the polar regions; more details and error estimates for the derivation of fluxes are given in Renfrew et al. (2002a,b).

3.5. Ice production modelling

Once a time series of the total surface heat flux, Q_{tot}, is obtained, it is weighted by the directly-observed open water fraction to derive the ocean cooling. This enables quantification of the rate of ice production, via:

$$Q_{tot} = \rho_i L_f F \quad (3)$$

where ρ_i is the density of ice, L_f is the latent heat of fusion, and F is the time-dependent ice production rate. An assumption is made that ice is produced only when Q_{tot} is positive (heat flux from ocean to atmosphere). Further, it is assumed that ice is only produced during the period 1 May to 1 November, outside of which a surface heat loss would lead to ocean cooling rather than ice production (see Meredith et al. (2004)) for further details and justification of this assumption). A simple relationship (derived locally) between ice fraction and ice thickness is used to account for the latter in the heat flux weighting, as per Renfrew et al. (2002a), and as described in Meredith et al. (2004). Note that the ice production calculated here for the earlier years differs slightly from that calculated in previous works (e.g. Meredith et al. (2004)) because of different weightings given to the individual sea ice types in deriving overall concentration. These minor differences (~0.1 m) in ice production estimates do not affect the conclusions of this or previous studies.

3.6. Climatic indices and data

The SAM index used here is that of Marshall (2003), available at http://www.nerc-bas.ac.uk/icd/gjma/sam.html. For ENSO, the Niño3.4 index of Cane et al. (1986) is used, consisting of sea surface temperatures averaged over 5°N to 5°S and 170–120°W. Sea level pressure data are from the National Center of Environmental

Prediction and National Center for Atmospheric Research Reanalysis (NNR) project (Kalnay et al., 1996). Here we used post-1978 NNR sea level pressure data, when the introduction of satellite data into the numerical data analysis indicated marked improvements for the Southern Ocean (Marshall and Harangozo, 2000). Further, comparisons of NNR sea level pressures with data from other reanalysis projects show similar results (e.g. Bromwich et al. (2007)). WAP sea level pressures were derived here as the average over the region 60–70°S and 65–100°W. The Niño3.4 index and the NNR sea level pressure data were obtained from http://iridl.ldeo.columbia.edu.

4. Results

4.1. Vertical profiles

The time sequence of full-depth profiles of salinity and $\delta^{18}O$ at the RaTS site is shown in Fig. 4. Three of these profiles (December 2001–2003) were shown previously (Meredith et al., 2008a); here we extend this sequence up to 2007, and also add some previously-collected profiles. It is immediately obvious that the spread of both salinity and $\delta^{18}O$ in the upper ocean shown is much larger than in the profiles presented previously; in particular the March 1999 and February 2006 profiles are significantly fresher and isotopically lighter at the surface compared with the period December 2001–2003. (We stress here that this difference reflects more the timing of the sampling within the year, rather than the difference between years; this aliasing issue is discussed in more detail below). The fresher and isotopically lighter nature of the March 1999 and February 2006 data is indicative of extra addition of meteoric water prior to sampling at these times, since if the fresher water were due solely to the presence of more sea ice, it would only have a significant signal in the salinity profiles rather than both salinity and $\delta^{18}O$.

This is demonstrated more quantitatively in Fig. 5, which shows the result of the three-endmember calculation (Eq. (1)) when applied to these data. The December profiles (2000–2003) show maximum meteoric water concentration at the surface of around 3%, whereas the profiles collected in other years show maximum meteoric water concentrations at the surface of typically 4–4.5%. Sea ice melt concentrations are also different, with the December profiles showing values around −0.5% or less, whereas the other profiles have surface values around 0–1%. (Note that a negative sea ice melt is indicative of there having been a net sea ice formation from the water prior to it being sampled.)

Column inventories of the freshwater components were derived by vertically integrating the profiles shown in Fig. 5. (A base of 260 m was used for this integration; this is a reasonable common level above which the freshwater of interest is generally constrained.) The results of this are shown in Fig. 6, with the horizontal axis denoting both the month and year of the profile collection. It is clear that the years when the sampling was conducted in December and January have the lowest column inventories of meteoric water (around 4 m), with sampling at other times have significantly higher inventories (maximum of over 6 m in March 1999). Sea ice melt was also at its most extreme in March 1999, with a value of around −1.5 m. Accounting for the difference in density between sea ice and water, this is indicative of around 1.6 m of sea ice having formed from this water column prior to it being sampled. Other values are less extreme, typically lying in the range −1 to −0.5 m for December 2001–January 2005, though peaking at around 0.5 m in February 2006.

When using data from a single location, there is inevitably a question concerning how representative this data is of the larger area in which it sits. We cannot answer this question definitively, however some insight can be gained by examining data from the broader region of Marguerite Bay, albeit collected at essentially a single point in time. Fig. 7 shows the spatial distribution of the column inventories of meteoric water, as determined from samples collected during cruise JR137/150 in February 2006. One station was conducted at the RaTS site adjacent to Adelaide Island, other stations were conducted in and around the entrance to Marguerite Bay. The column inventory for meteoric water at the RaTS site was 4.8 m; other stations had a root-mean-square difference from this of 0.6 m. This is somewhat lower than the approximate error in derivation of the column inventories (around 1 m, derived from a combination of measurement uncertainty, error due to sparse vertical sampling and error in determining the freshwater percentages due to uncertainties in endmembers, including that of CDW).

The corresponding spatial distribution of sea ice melt from the same cruise is shown in Fig. 8. At the time of the cruise, the RaTS site had a column inventory of 0.4 m, with other stations having a root-mean-square difference from this of 0.7 m. Sea ice melt derived using Eq. (1) can be positive or negative (depending on previous net sea ice melt or formation), and this is seen in the spread of values in Fig. 8. As with meteoric water, however, the root-mean-square difference in sea ice melt from the value at the RaTS site is lower than the error in its calculation.

Overall, the cruise data place useful constraints on how representative the RaTS data are with regard to the broader Marguerite Bay area, and whilst the differences between the stations are not insignificant (due partly to the complex eddy field on this part of the WAP shelf (Beardsley et al., 2004)), the general patterns give us some confidence that the RaTS profile data, whilst coming from a coastal site, do have a level of broader relevance. In particular, the dominance of the freshwater budget by meteoric water in summer is confirmed across the region of northern Marguerite Bay. It is worth noting also that the timing of the JR137/150 cruise was in austral summer, when glacial ice melt from the coast is likely to be close to its maximum, and hence across-shelf gradients in meteoric water (which is dominated by glacial ice melt here (Meredith et al., 2008a)) are likely to be highest. Consequently, the level of representativeness for meteoric water seen from this individual cruise is likely to be a conservative estimate of the overall representativeness of the data.

4.2. Time series at 15 m depth

With regard to our derived time series of column inventories of freshwater (Fig. 6), it is important not to view this temporal pattern as denoting a sudden reduction in freshwater prevalences soon after March 1999, followed by a steady recovery. Instead, it needs to be borne in mind that the profiles during the middle part of the series were collected during earlier months in the austral summer (December and January), while those at the start and end of the sequence were collected during later months in the summer (February–April). There is thus the potential for significant aliasing of seasonal variability, and its misinterpretation as interannual variability. Indeed, this must reflect at least some of the variability seen, and probably most. Consequently, sampling at a higher frequency is needed to avoid aliasing problems, and to better address the interannual changes in freshwater input to the WAP ocean.

Although we cannot quantify column integrals of freshwater from our quasi-weekly RaTS sampling at 15 m, this dataset does provide sufficiently high temporal resolution to avoid seasonal aliasing and misinterpretation of the interannual signals. Fig. 9 shows the time series of potential temperature, salinity, and $\delta^{18}O$ at 15 m depth at the RaTS site. Also shown is mixed layer depth (MLD, here defined as the depth at which the water is 0.05 kg m^{-3} denser than the surface water at that time), derived from the full-depth CTD

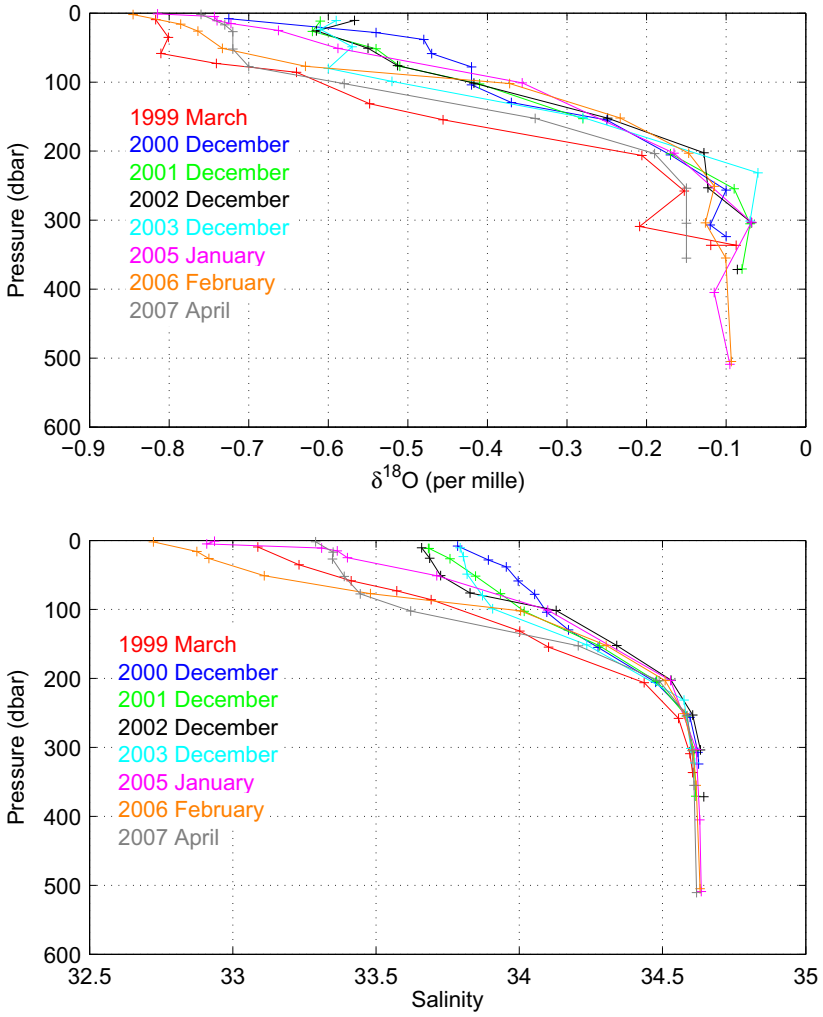

Fig. 4. Profiles of (top) $\delta^{18}O$ and (bottom) salinity at the RaTS site (Fig. 2) collected during visits of *RRS James Clark Ross* to Rothera in the austral summer. Profiles are colour-coded by date. Note that the fresher upper-layer waters are also isotopically lightest, denoting significant input of freshwater of meteoric origin.

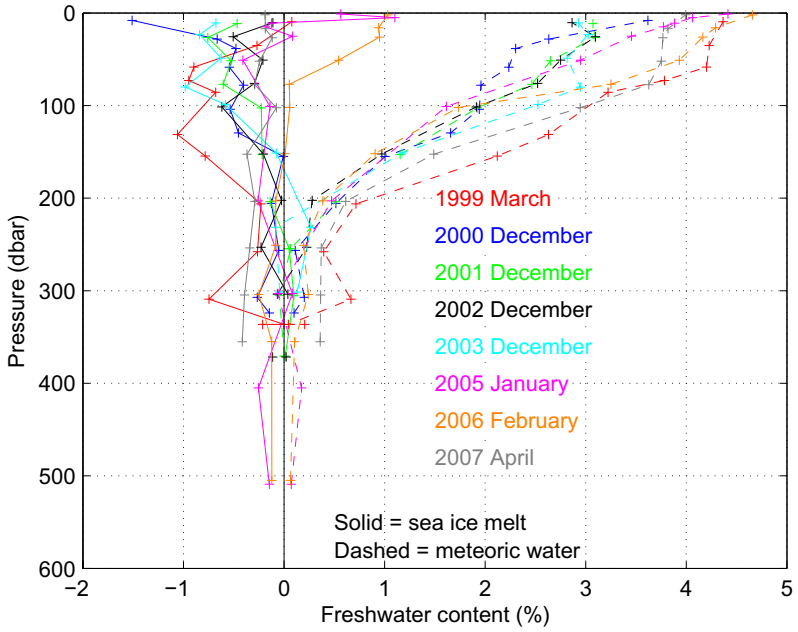

Fig. 5. Vertical profiles of sea ice melt (solid) and meteoric water (dashed) calculated from the profiles shown in Fig. 4. Profiles are colour-coded by date; approximate uncertainty is around 1%. Negative values for sea ice melt indicate there having been a net sea ice formation from these waters prior to them being sampling.

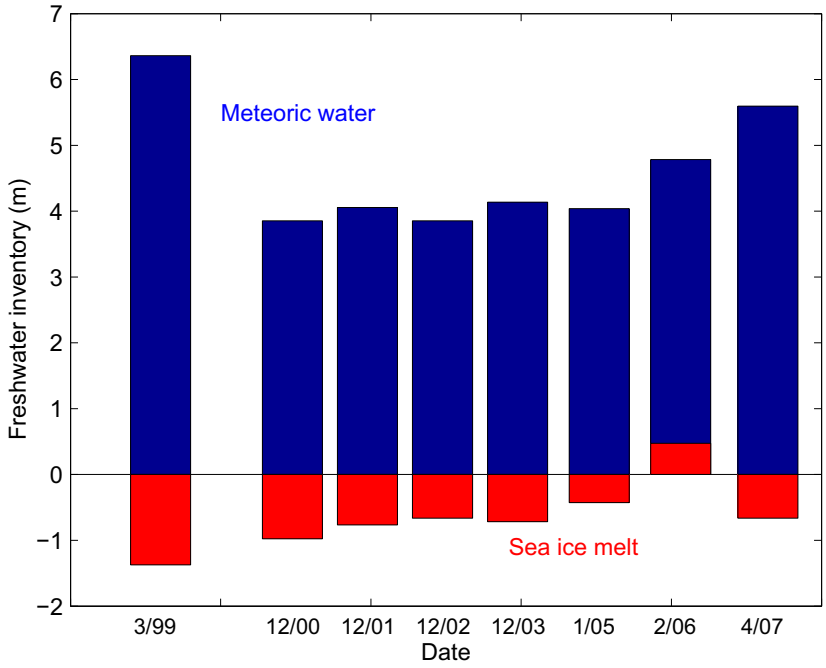

Fig. 6. Column inventories of meteoric water (blue) and sea ice melt (red) at the RaTS site as a function of time. Approximate uncertainty is around 1 m. Date is labeled as month/year.

profiles conducted during RaTS events. The first 2 years of this dataset were presented previously and the seasonal variability discussed (Meredith et al., 2008a); here we update the record to nearly present-day, and focus on the interannual signals.

Significant interannual variability is apparent in these series. For example, the highest salinity ($S > 34$) was observed around October 2007, coinciding with the isotopically heaviest water measured ($\delta^{18}O > -0.4‰$). The freshest water occurred during March 2006 (around 32.2), and whilst $\delta^{18}O$ showed that isotopically light waters were present at this time, they were no lighter than in the same months in many other years. 2007 showed a very large range in $\delta^{18}O$ from summer to winter, around twice that of a typical year.

To better understand the physical processes behind the interannual changes in the 15 m time series, we here investigate the data in salinity-$\delta^{18}O$ space (Fig. 10). When considered this way, sea ice processes affect the loci of data points in a near-horizontal sense, with melt moving the points to the left, and freezing moving the points to the right. Mixing with CDW affects both salinity and $\delta^{18}O$, and moves the loci upwards and to the right. Conversely, addition of meteoric water affects both salinity and $\delta^{18}O$ in the opposite sense, moving the loci downwards and to the left. In Fig. 10, the envelope of salinity-$\delta^{18}O$ space that could be inhabited purely under conditions of mixing with CDW or meteoric water is bounded by the dashed straight lines; consequently, data points that lie outside this envelope show significant influence from sea ice processes. (The two outermost dashed lines in Fig. 10 represent extrapolations to reasonable maximum and minimum values for meteoric water input at the WAP (Meredith et al., 2008a); the middle dashed line is a median between these.)

Years where sea ice formation exerted the most obvious influence on the data include 2002, 2004 and 2008; in each of these, data points are clustered outside the envelope of dashed lines between meteoric water and CDW. The most conspicuous event of strong sea ice meltwater input (seen here as data points clustered farthest to the left outside the envelope of dashed lines) is during 2005. The most significant influence of CDW occurs in 2007 (cluster of points closest to the top right of the panel), whilst the greatest influence of meteoric water occurred in 2006 (cluster of points farthest to the lower left in the panel). An important point to bear in mind when interpreting these freshwater loci is that multiple processes that occur at the same time can have subtle impacts. For example, if ice production influences the upper ocean, it will move the cluster of points to the right in salinity-$\delta^{18}O$ space, but if this formation also induces more mixing with CDW, the additional diagonal movement of the cluster (upwards to the right) may partially obscure the apparent strength of the ice formation. This interaction is investigated in more detail below.

To interpret our 15 m series more quantitatively, we use the three-endmember mass balance calculation (Eq. (1)) to derive the time-dependent fractions of meteoric water, sea ice melt and CDW (Fig. 11). Meteoric water varies greatly, from nearly 6% in March 2006 and 2007, to less than 2% in October 2007. This is a much greater range than derived from the shorter series investigated previously (Meredith et al., 2008a). Sea ice also has a much larger range than derived previously, with a maximum of over 2% in February 2005, and a minimum of close to −2% July 2002. The maximum sea ice melt prevalence (February 2005) took the form of a narrow peak, indicative of a comparatively sudden pulse of melt, however there are several data points within this peak and we can be confident it is not an artefact of data quality. The sea ice melt curves are particularly flat during the years 2003, 2007 and 2008, with other years showing more pronounced seasonal cycles.

CDW shows highest prevalences in October and November 2007 (though matched by a couple of data points in 2002), and minimum prevalence in March 2006. Clearly the nature of the three-endmember calculation used forces CDW to be the balancing term for the totality of the waters present (which must total unity; Eq. (1)). However, for periods such as October 2007 (which had high CDW prevalence, and saline and isotopically heavy waters at 15 m, reflected as record-low meteoric water concentrations), the physical interpretation must be that more CDW had mixed vertically to 15 m depth than in other years.

In terms of explaining the interannual variability observed in the freshwater components at 15 m depth, a particularly strong

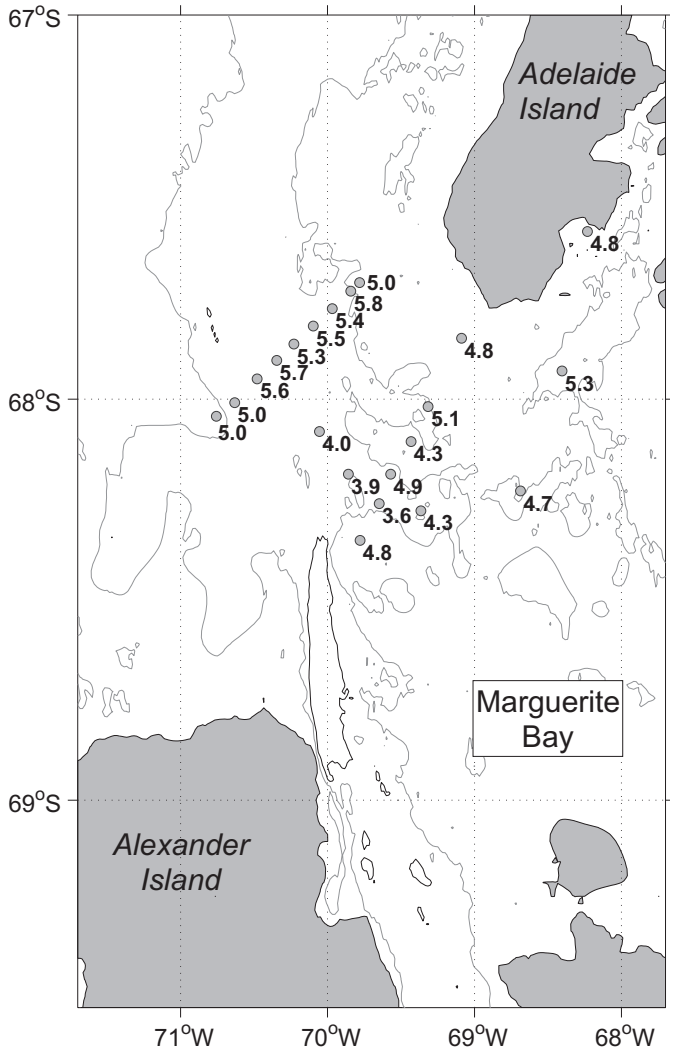

Fig. 7. Column inventories of meteoric water, derived from salinity and $\delta^{18}O$ data collected during *RRS James Clark Ross* cruise JR137/150 in February 2006. One station is at the RaTS site adjacent to Adelaide Island, other stations were conducted in and around the entrance to Marguerite Bay. The column inventory for meteoric water at the RaTS site was 4.8 m; other stations had a root-mean-square difference from this of 0.6 m. The 500 m and 1000 m isobaths are plotted.

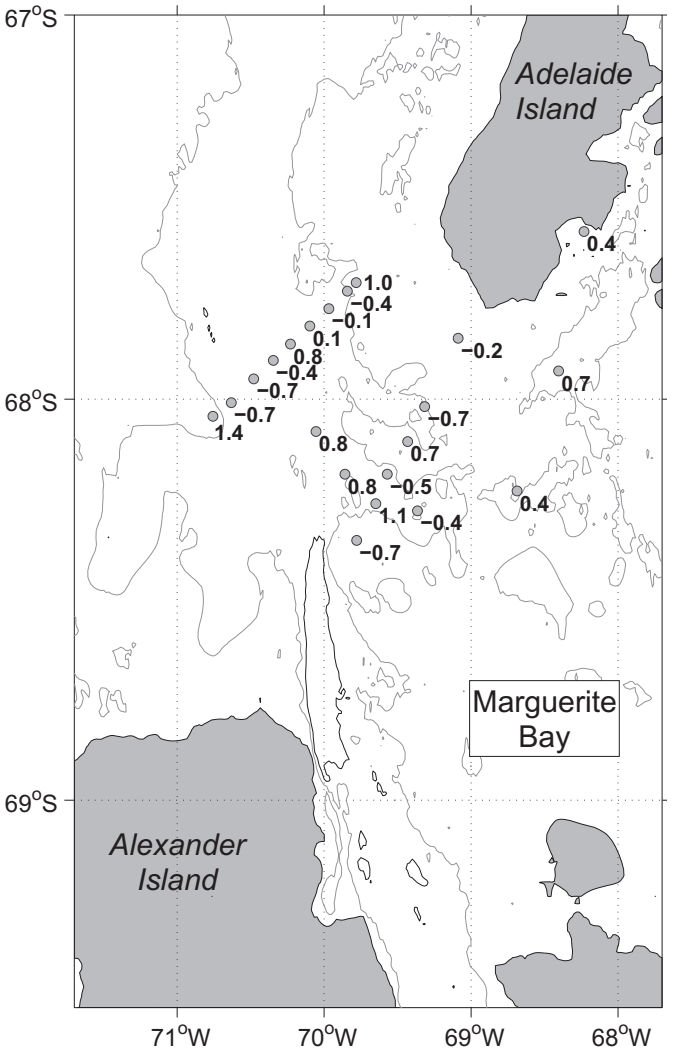

Fig. 8. As for Fig. 7, but for sea ice melt rather than meteoric water. The RaTS site had a column inventory of 0.4 m at the time of sampling; other stations had a root-mean-square difference from this of 0.7 m. The 500 m and 1000 m isobaths are plotted.

influence appears to be changes in the winter MLD. During our sequence of measurements, there are three particularly strong examples of deep mixed layers during winter, namely 2003, 2007 and 2008 (Fig. 9), when MLDs reached close to 200 m for the former two events, and around 120 m for the latter. By comparison, other years had much shallower mixed layers in winter, with MLDs of around 50 m or less.

Years with deeper mixed layers clearly have the potential to mix more CDW upwards into the mixed layer (Smith and Klinck, 2002; Meredith et al., 2004; Martinson et al., 2008), with the effect of reducing the prevalences of the freshwater components present. This is an obvious explanation for the very flat sea ice melt curves in 2003, 2007 and 2008, and the reduced meteoric water content at 15 m in the winters of these years (Fig. 11). However, this is not a simple pattern of cause and effect, with MLD affecting the freshwater budget. Previously it was argued that the largest single determinant for MLD changes at the WAP was the time-varying rate of sea ice production (Meredith et al., 2004; Smith and Klinck, 2002), and other terms in the freshwater budget also have the potential to influence MLD. Clearly there is a need to understand in more detail the causes of the deep mixed layers in our current sequence of data, so as to better elucidate their climatic forcings and their impacts on the freshwater balance.

4.3. Meteorological forcing and sea ice production

To understand the causes for the interannual changes in freshwater and upper-ocean structure, we here examine the meteorological forcings and sea ice production calculated as per Section 3. It is notable that the years 2003, 2007 and 2008 were anomalously warm (as indicated by mean air temperature; Table 1), with relatively strong vector mean NNE-NE winds. The impact that these factors have on the local sea ice field is profound. Fig. 12 shows the time series of observed ice score, and it is clear that 2003, 2007 and 2008 were all years with low or very low sea ice cover in winter. This was especially the case in 2007 and 2008. Other years showed much more persistent sea ice cover, with 2002 being an extreme example, when complete fast ice cover persisted from mid-May to December.

As a consequence of the greatly reduced sea ice cover in 2003, 2007 and 2008, a much greater fraction of the ocean was exposed to the atmosphere during winter. This enabled much greater integrated air-sea heat fluxes, and consequently much larger amounts

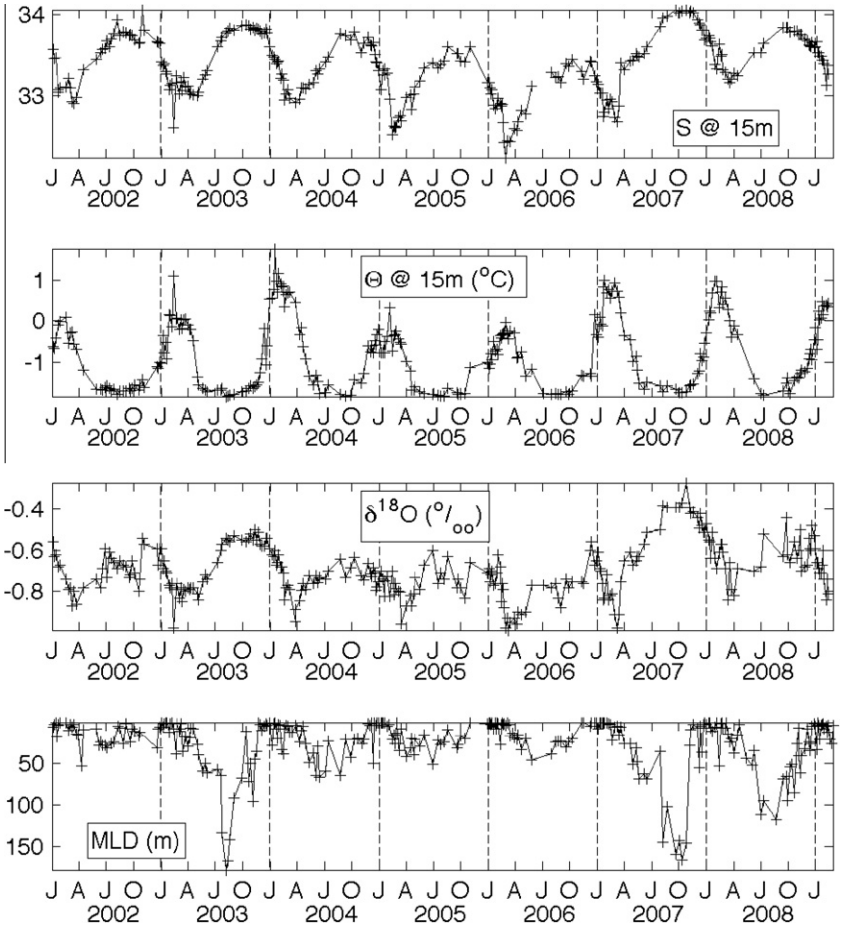

Fig. 9. Time series of salinity, potential temperature, $\delta^{18}O$ and mixed layer depth (MLD) at 15 m depth at the RaTS site as a function of time. MLD is here defined as the depth at which the water is 0.05 kg m^{-3} denser than the surface water at that time. The starts of the months January, April, July and October are marked for each year.

of sea ice production (Fig. 13). Ice production is a key mechanism for creating deep mixed layers at the WAP, via brine rejection and buoyancy loss in the upper ocean, and if the ice production is sustained, these waters can convect to much deeper levels. We have argued previously that a very deep mixed layer observed in northern Marguerite Bay in 1998 was created via this mechanism (Meredith et al., 2004), with anomalous northerly winds acting to persistently move the sea ice southward away from Adelaide Island, resulting in unusually low sea ice conditions, strong air-sea fluxes, and consequently very strong ice production.

It seems highly likely that this same process is a key contributor to the deep mixed layers in 2003, 2007 and 2008, and hence is a critical factor in modulating the freshwater content of the upper ocean at these times. Notwithstanding this, however, it must also be borne in mind that the reduced sea ice cover in these years will have led to markedly stronger wind stress impacting on the ocean. There were high levels of such wind stress "felt" by the ocean in 2003, 2007 and 2008 (Table 1), leaving open the possibility that directly wind-induced mixing may also play a role in homogenizing the upper ocean at the RaTS site in years of low ice cover. This is discussed more below.

4.4. Climatic forcing of northern Marguerite Bay

We have seen that changes in meteorological forcing and sea ice production on interannual timescales can strongly affect the freshwater composition of the upper ocean in northern Marguerite Bay, both directly (by impacting on the amount of freshwater extracted from the ocean as sea ice), and indirectly (by influencing the depth of the mixed layer, and hence the level of CDW mixing into the upper ocean). To understand the climatic causes of the interannual changes in meteorological forcing, and thereby enhance the likelihood of generation of predictive skill, we need to elucidate the large-scale atmospheric forcings over the WAP in relation to our time series of measurements.

As illustrated in Fig. 3, during La Niña or positive SAM events, there are negative atmospheric pressure anomalies in the high latitude southeast Pacific (and vice versa for El Niño or negative SAM events). Cyclonic (anticyclonic) flow associated with the low (high) pressure anomaly would contribute to increased northerly (southerly) winds over the WAP during La Niña (El Niño) and/or positive (negative) SAM events. Thus, the coincident phasing of these two atmospheric modes has the potential to amplify or dampen the atmospheric circulation anomaly (Fogt and Bromwich, 2006; Stammerjohn et al., 2008b) and the consequent meridional wind anomalies over the WAP.

To investigate the potential impact of these two atmospheric modes, time series of the SAM and ENSO indices are shown together with WAP sea level pressure over 2002–2008 (Fig. 14). As described by Stammerjohn et al. (2008a) (see their Fig. 7 and related discussions in particular), during positive (negative) SAM conditions, there are negative (positive) sea level pressure anomalies in the WAP area, the magnitude of which depend in part on ENSO, e.g. amplified negative (positive) sea level pressure anomalies during positive SAM/La Niña (negative SAM/El Niño), such as was the case in late 2007–2008 (2002). Several studies have shown that during anomalously low sea

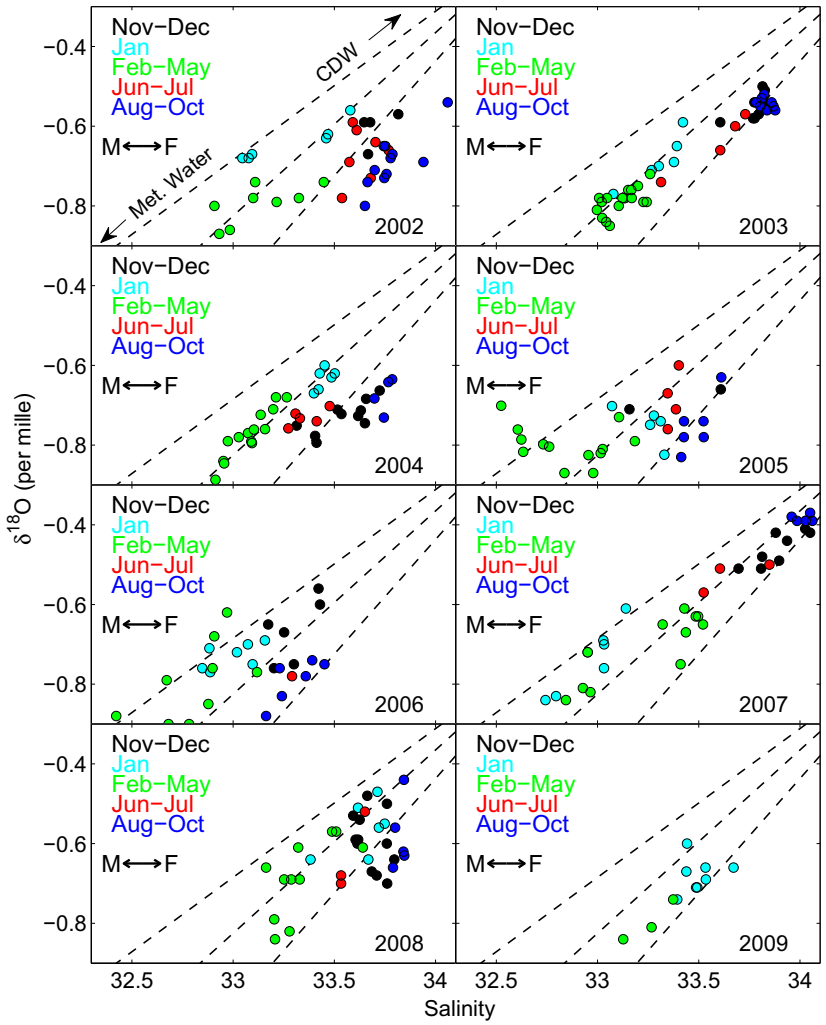

Fig. 10. Freshwater loci for 2002–2009. Data points are from individual samples collected at 15 m depth at the RaTS site. Separate panels are for the years marked; data points are colour-coded by month. (The colour-coding is irregular, with the choice of groupings made to highlight the processes occurring at different times of year.) In the salinity-δ^{18}O space used here, melting and freezing (marked M-F) would move the data points almost horizontally. Mixing with CDW would move the data points diagonally upward to the right, within the envelope of the dashed straight lines. Mixing with pure meteoric water would move the data points diagonally down to the left, again with the envelope of the dashed lines. (Dashed lines are derived from extrapolations between zero salinity endmembers with reasonable minimum and maximum δ^{18}O values for meteoric water input at the WAP, and reasonable upper and lower limits for CDW properties, with a median line also added.)

level pressure conditions (late 2007 and 2008), warm northerly winds prevail over the WAP region in conjunction with strong cyclonic atmospheric conditions, while during anomalously high sea level pressure conditions (2002), cold southerly winds prevail over the WAP region in conjunction with anticyclonic atmospheric conditions (e.g. Marshall and King (1998), Massom et al. (2008), Stammerjohn et al. (2008a)).

Clearly for the 2002–2008 time period, the largest SAM, ENSO and WAP sea level pressure values occurred when SAM and ENSO interfered constructively (i.e. when their indices correlated negatively) as illustrated by the negative SAM/El Niño of 2002 and the sustained positive SAM/La Niña from late 2007 to 2008. For the intervening years, WAP sea level pressure is negatively correlated with SAM as expected, but the magnitude of the sea level pressure anomaly (as well as the magnitude of the SAM index) is diminished compared with 2002 and 2007–2008. During this period the phases of SAM and ENSO are positively correlated, and thus interfere destructively, which may explain the relatively weaker index values. There are two notable short-term exceptions however (i.e., based on unsmoothed data in Fig. 14b), the anomalously low WAP sea level pressure in mid-winter 2003 and 2007. The former coincides with a short-term positive SAM event but an otherwise neutral ENSO conditions. The latter coincides with the onset of a strong La Niña in mid-2007. The meridional wind anomalies that occurred in 2003 are therefore ascribed to a positive SAM state during late autumn and mid-winter that year. In contrast, during 2007, the increase in winds that started in August was associated with the onset of strong La Niña conditions, supplemented by positive SAM late in the year. During 2008, positive SAM/La Niña conditions prevailed during the early part of the year, with the positive SAM contributing into the latter part also. These patterns of large-scale climate variability are the drivers for the anomalous northerly winds over the WAP in these years, and hence for the patterns seen in the sea ice and upper ocean measurements.

5. Discussion and conclusions

We have used a combination of salinity and oxygen isotope data from a near-coastal site at the Antarctic Peninsula to investigate freshwater variability and upper-ocean stratification changes in response to climatic variability. We have confirmed the predominance

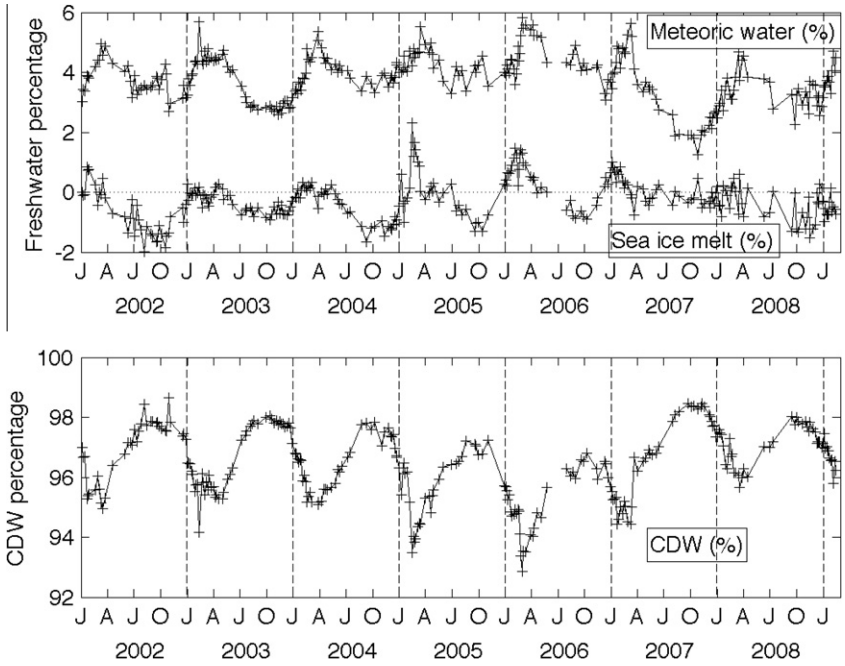

Fig. 11. Time series of (top) meteoric water and sea ice melt, and (bottom) CDW at 15 m depth at the RaTS site.

Table 1
Selected meteorological data from Rothera for each year for which we have $\delta^{18}O$ data. Data are means for the period June–August, except for the last two columns which are annual averages.

Year	Air temp. (°C)	Wind speed ($m\ s^{-1}$)	Vector-mean wind speed ($m\ s^{-1}$)	Vector-mean wind direction	Mean-sea-level pressure (mbar)	Annual ice production (m)	Annual mean wind stress felt by the ocean ($N\ m^{-2}$)
2002	−13.76	5.85	2.81	7.0	994.1	1.12	0.034
2003	−7.44	7.17	3.77	18.1	984.4	3.16	0.092
2004	−8.71	7.06	3.42	358.9	986.5	2.13	0.071
2005	−10.78	5.80	2.98	11.7	993.5	0.79	0.043
2006	−9.87	5.50	2.81	3.7	995.4	1.70	0.064
2007	−8.26	6.86	3.16	67.0	989.6	4.66	0.100
2008	−7.54	7.17	3.94	27.2	989.1	3.08	0.108

of meteoric water inputs over those of sea ice melt, in accord with previous findings, but the range of both is considerably larger than previously stated (the peak-to-peak range in meteoric water range is 5%, and that of sea ice melt range is 4%. These contrast with previous values of 2–3% for each given previously (Meredith et al., 2008a), and are a reflection of the strong interannual variability in both series).

A perennial problem with time series data is the need to establish the spatial scales over which the record is representative. This is a particular issue for us, since our time series is from a near-coastal site, where the spatial gradients could be larger than average due to processes associated with runoff and topographic effects. Whilst we cannot address this question definitively, we have nonetheless made some progress by considering the spatial distribution of column inventories of meteoric water and sea ice melt across the northern part of Marguerite Bay and westward toward the broader WAP shelf in February 2006. The summertime predominance of meteoric water in the freshwater budget is confirmed, with sea ice melt constituting a much smaller percentage of the overall freshwater content. In this context, it is worth noting that the seasonality of the meteoric water is likely to be highest near the coast, since it is dominated by glacial runoff (Meredith et al., 2008a). Consequently, this gives our RaTS time series the unintended advantage of providing a useful upper limit to the seasonality in meteoric water content that is likely to be observed across the broader WAP shelf away from the coast.

In terms of the interannual variability observed, the years 2003, 2007 and 2008 had notably small ranges in sea ice melt, and also low meteoric water percentages during winter and spring. These years also featured very deep winter mixed layers, and we argue here that this is not coincidental. Calculations of sea ice production show strongest values in these years, due to the weak sea ice cover allowing strong air-sea heat fluxes to persist through the winter, and strong ice production to progress uninhibited. The lack of sea ice cover is related to anomalously persistent northerly winds in each of these years, which acts to push the ice southward as it forms, and keep northern Marguerite Bay relatively ice free. The strong ice production creates deep mixed layers that excavate downwards into the underlying CDW. The CDW is then distributed over the full vertical extent of the mixed layer, and reduces the freshwater fractions measured at 15 m, hence diminishing the meteoric water percentages and constraining the sea ice melt percentages to be closer to zero.

With the instances seen here, and a previous occurrence in 1998 (Meredith et al., 2004), it seems that these deep mixed layers caused by anomalous meteorological and cryospheric forcing are a recurring (but aperiodic) phenomenon in northern Marguerite Bay. Climatic forcing from both SAM and ENSO contributes to the anomalous northerly winds (in particular via periods of sustained positive SAM and/or La Niña conditions), and hence the deep mixed layers and associated redistribution of freshwater over a greater vertical range.

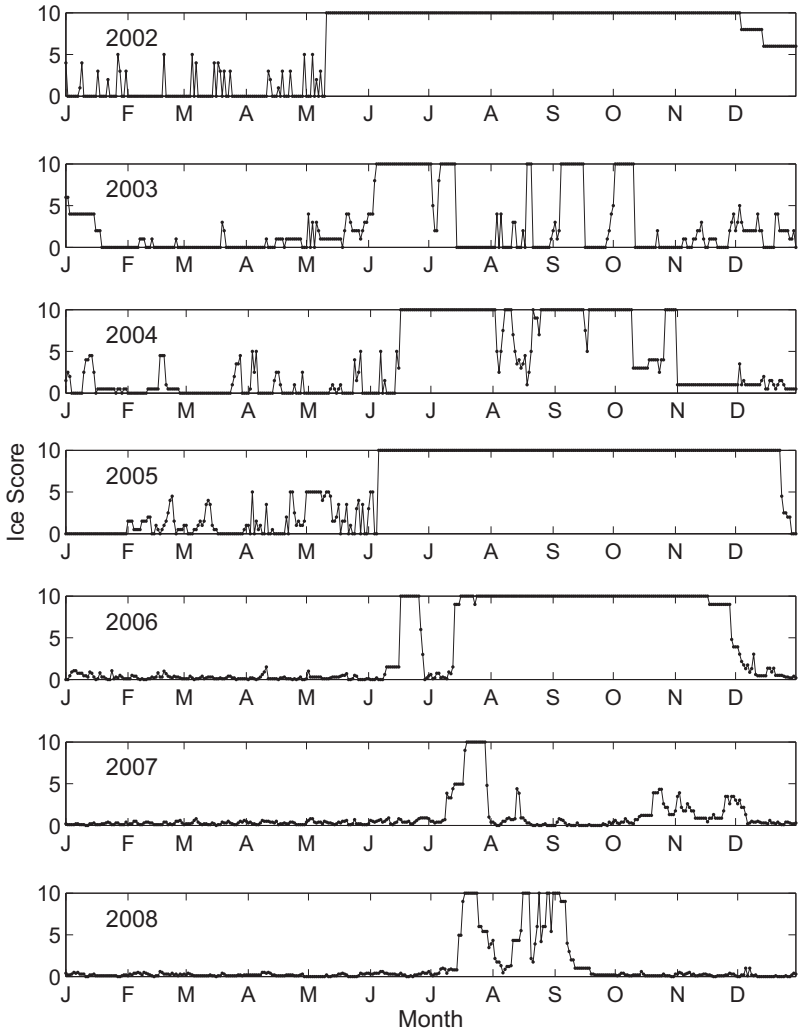

Fig. 12. Ice score close to the RaTS site, calculated from direct observations using a weighted average of different ice types and concentrations.

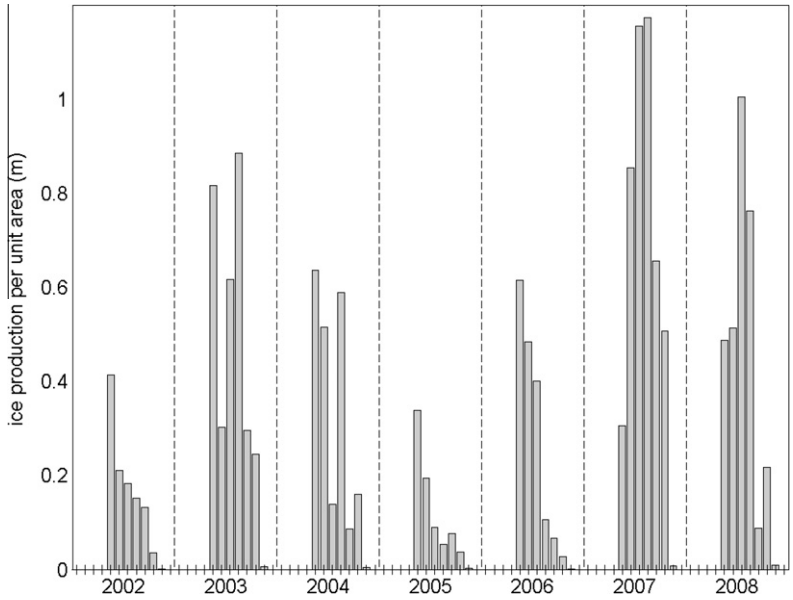

Fig. 13. Sea ice production at Rothera, calculated as per Renfrew et al. (2002a,b). Note in particular the strong values in 2003, 2007 and 2008, coincident with the occurrence of deep mixed layers in winter.

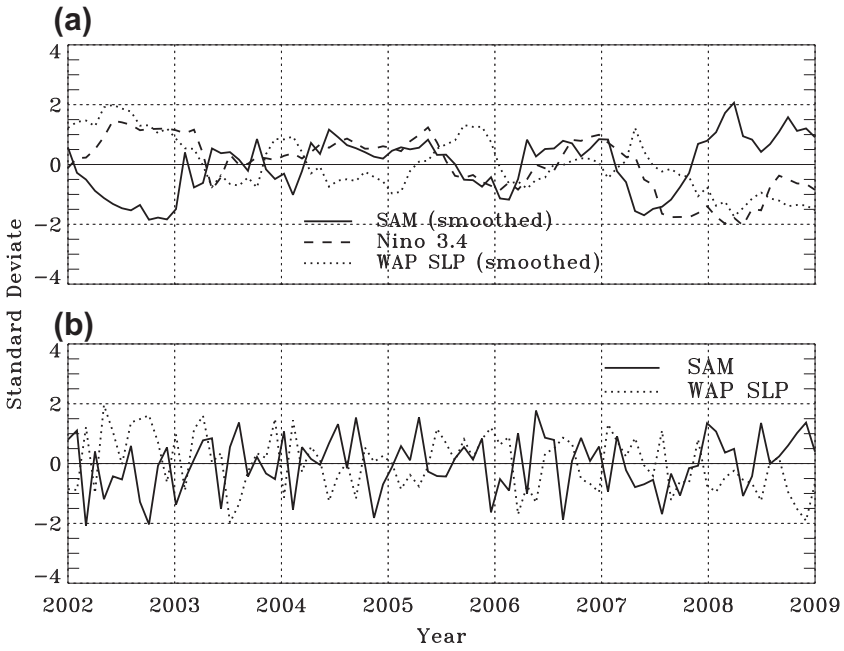

Fig. 14. (a) Monthly time series of the (smoothed) SAM index (solid), Niño 3.4 index (dashed) and (smoothed) WAP sea level pressure (SLP; dotted) over 2002–2008. The SAM and WAP SLP were smoothed with a 7-month running mean filter. (b) Monthly time series of the SAM index and WAP SLP (unsmoothed). All time series are monthly anomalies normalised by the standard deviation.

It is worth noting that, following winters with deep mixed layers and hence less negative sea ice melt percentages, the peak sea ice melt the following summer tends to be reduced. Most notably, the summers of 2004, 2008 and 2009 (following the winters with deep mixed layers in 2003, 2007 and 2008) have low sea ice melt percentages in January and February, especially compared with e.g. the large peaks seen in 2005 and 2006. Conversely, the years with the strongest sea ice melt percentages in summer (2002, 2005, 2006 and 2007) all follow winters that did not exhibit deep mixed layers. This suggests that the process of restratification of the ocean following a winter with weak ice coverage and a deep mixed layer is delayed and reduced, and leads to some persistence in the reduced extrema in freshwater content of the near-surface ocean. The most likely mechanism to explain this is sea ice advection, whereby the persistent northerly winds that characterise winters with deep mixed layers can have a dual effect: initially to enable strong ice production and the formation of the deep mixed layer over which freshwater anomalies are spread, but also to advect sea ice away from the southern coast of Adelaide Island, where its subsequent melt cannot contribute to local restratification of the upper ocean the following spring and summer.

With seasonal mixed layer processes being seen to be a key factor in controlling the near-surface freshwater balance, it is worth exploring in more detail the mechanisms that control MLD changes on interannual timescales. Previously, we used a one-dimensional mixed layer model (based on Price et al. (1986)) to demonstrate that sea ice production and the increase in upper-layer density is likely to be the most important factor controlling MLD (Meredith et al., 2004). This is in accord with other modelling studies of the broader WAP region (Smith and Klinck, 2002), and the temporal correspondence seen here of deep mixed layers with years of weak sea ice cover and high rates of sea ice production all support this interpretation. However, it is worth noting that this may not be the only important process in the formation of the deep winter mixed layers at the RaTS site.

RaTS is conspicuously close to a coastal boundary (Fig. 2), and recent findings indicate that wind-induced upwelling and downwelling and internal tides can induce significant anomalies in hydrographic characteristics here (Wallace et al., 2008). Direct quantification of mixing via these processes requires further measurements to be made, however they will almost certainly induce a level of vertical mixing above that present in the WAP ocean away from the topographic boundary. Wallace et al. (2008) demonstrated that these processes were more energetic during times of weak or absent sea ice, and consequently could contribute to a deep winter mixed layer more readily in years with low sea ice cover. Accordingly, we speculate here that the deep winter mixed layers created by sea ice production in northern Marguerite Bay are enhanced locally by wind-induced coastal processes, and which are stronger in ice-free seasons than during periods of heavy ice cover. A previous investigation (Meredith et al., 2004), which did not take account of this possibility, used a one-dimensional mixed layer model to determine the processes controlling winter mixed layer depth; however, this model was configured for a generic water column on the WAP shelf, and coastally-enhanced processes were not represented.

It is worth noting that to balance large-scale budgets of heat and salt on the WAP shelf requires a level of mixing that has not been observed on research cruises (Smith and Klinck, 2002), leading to the speculation that the key sites for mixing are shallow regions and/or coastal locations that are not frequented by research vessels (Howard et al. (2004), Wallace et al. (2008); L. Padman, pers. comm.). The notion we have put forward here, of wind-driven coastal processes enhancing upper-ocean mixing, is consistent with the northern Marguerite Bay region being one of significant mixing. This has important ecological consequences, not least because of the enhanced supply of heat and nutrients to the mixed layer that would occur here.

In terms of understanding the processes of change at the WAP and their consequences for the ecosystem, it was shown recently for the southern WAP region that decreases in sea ice were associated with increases in water column stratification (Montes-Hugo et al., 2009). (Combined with decreases in cloud, these led to an increase in phytoplankton biomass, with consequences for higher trophic levels including zooplankton and penguins (Montes-Hugo et al., 2009).) In a mechanistic sense, the processes we have

observed at the RaTS site produce the opposite result: we find that years with reduced sea ice concentrations are associated with a decrease in water column stratification (deeper mixed layers) during winter, and weaker restratification the following spring/summer. This difference is very likely to be a reflection of the locality of RaTS in northern Marguerite Bay, and its tendency for polynya-like behaviour.

The climatic drivers for the main interannual changes seen here have been identified as SAM and ENSO, via their impacts on northerly winds at the WAP. Both of these climate modes have shown marked long-period changes in their behaviour in recent decades, with SAM showing a trend to a more positive state (stronger circumpolar winds), and ENSO showing a greater preponderance of El Niño events compared with La Niña events (Thompson et al., 2000; Marshall, 2003; Turner, 2004). The SAM trend has been attributed partly to anthropogenic influences (Thompson and Solomon, 2002; Gillett and Thompson, 2003; Marshall, 2003), whilst that of ENSO is under debate. If such trends continue, the relationships observed here could potentially be used to develop some predictive skill in how the upper ocean in northern Marguerite Bay may respond. In particular, if the trend toward more positive SAM conditions continues, there are likely to be more frequent occurrences of anomalous northerly winds at the WAP, with implications for mixed layer depths, freshwater distributions and the ecosystem. This could be countered by a potential continuing trend toward a greater frequency of El Niño events (compared with La Niña events). Determining the future time-varying balance between the two could be key in predicting the evolving physical/ecological system in Marguerite Bay and across the WAP ocean.

In general terms, our presumptions at present are that glacial melt at the WAP will increase in future decades, following the increases seen here recently (Cook et al., 2005), and that sea ice production over the broad WAP region will continue to decrease for some time, with less seasonality in the sea ice prevalence curve as a result (i.e. a late autumn advance, as described by Stammerjohn et al. (2008b), translating to less ice production in autumn and winter, with less ice available to melt the following spring and summer). The impact of this change on sea ice processes at the RaTS site is unclear, but if ice concentration in winter continues to decrease and northerly winds become more prevalent, stronger ice production could be a local result, until such time as temperature effects on ice production become dominant. Indeed, if warming progresses to the point that ice production at the Peninsula becomes negligible, mechanical processes and different buoyancy fluxes will become responsible for determining the interannual changes in mixed layer depth. The likely impact of these at the RaTS site is currently unclear.

A further predicted consequence of global warming is an acceleration of the hydrological cycle, with increased precipitation at high latitudes. This, and further deglaciation in the region, could lead to stronger meteoric water inputs in the vicinity of the WAP. As well as adding stability to the upper ocean, this could have the effect of increasing the supply of micronutrients and hence influencing primary production, with consequences for each of the higher trophic levels. Continued monitoring of $\delta^{18}O$ at locations such as RaTS is needed to track these changes as they occur, and determine the influence of each of the freshwater constituent changes on the marine ecosystem.

Acknowledgements

We thank a long succession of Marine Assistants at Rothera who have undertaken vital fieldwork, often in difficult conditions, to obtain the data and samples used here. Alice Chapman, Jenny Beaumont, Raynor Piper, Andrew Miller, Paul Mann, Helen Rossetti and Alison Massey are all gratefully acknowledged. Much support from Rothera base staff is also gratefully acknowledged, including those who have helped with sampling and boating operations down the years. Carol Arrowsmith is thanked for analysis of the isotope samples. Carlos Moffat and Bob Beardsley are thanked for the schematic of WAP circulation. Sharon Stammerjohn grateful acknowledges support from Palmer LTER. This work is a contribution of the British Antarctic Survey Polar Science for Planet Earth programme.

References

Bauch, D., Schlosser, P., Fairbanks, R.G., 1995. Freshwater balance and the sources of deep and bottom waters in the Arctic Ocean inferred from the distribution of $H_2{}^{18}O$. Progress in Oceanography 35, 53–80.

Beardsley, R.C., Limeburner, R., Owens, W.B., 2004. Drifter measurements of surface currents near Marguerite Bay on the western Antarctic Peninsula shelf during austral summer and fall, 2001 and 2002. Deep-Sea Research II 51, 1947–1964.

Beardsley, R.C., Moffat, C., Padman, L., Muench, R., & Owens, W.B. (2007). US SO GLOBEC Hydrographic and Circulation Studies. GLOBEC International Newsletter, vol. 13, pp. 52–54.

Bracegirdle, T.J., Connolley, W.M., Turner, J., 2008. Antarctic climate change over the twenty first century. Journal of Geophysical Research 113. doi:10.1029/2007JD008933.

Bromwich, D.H., Fogt, R.L., Hodges, K.I., Walsh, J.E., 2007. A tropospheric assessment of the ERA-40, NCEP and JRA-25 global reanalyses in the polar regions. Journal of Geophysical Research 112.

Cane, M.A., Zebiak, S.E., Dolan, S.C., 1986. Experimental forecasts of El Niño. Nature 322, 827–832.

Cook, A.J., Fox, A.J., Vaughan, D.G., Ferrigno, J.G., 2005. Retreating glacier fronts on the Antarctic Peninsula over the past half-century. Science 308, 541–544.

Craig, H., & Gordon, L., 1965. Deuterium and oxygen-18 variations in the ocean and the marine atmosphere. In: Tongiorgio, E. (Ed.), Stable Isotopes in Oceanographic Studies and Paleotemperatures, Spoleto, pp. 9–130.

DeCosmo, J., Katsaros, K.B., Smith, S.D., Anderson, R.J., Oost, W.A., Bumke, K., Chadwick, H., 1996. Air-sea exchange of water vapour and sensible heat: the humidity exchange over the sea (HEXOS) results. Journal of Geophysical Research 101, 12001–12016.

Dierssen, H.M., Smith, R.C., Vernet, M., 2002. Glacial meltwater dynamics in coastal waters west of the Antarctic Peninsula. Proceedings of the National Academy of Sciences 99, 1790–1795.

Dinniman, M.S., Klinck, J.M., 2004. A model study of circulation and cross-shelf exchange on the west Antarctic Peninsula continental shelf. Deep-Sea Research II 51, 2003–2022.

Ducklow, H.W., Clarke, A., Dickhut, R., Doney, S.C., Geisz, H., Huang, K., Martinson, D.G., Meredith, M.P., Moeller, H.V., Montes-Hugo, M., Schofield, O., Stammerjohn, S.E., Steinberg, D., Fraser, W., 2010. Marine pelagic ecosystems: the West Antarctic Peninsula. In: Rogers, A., Johnston, N., Clarke, A., Murphy, E. (Eds.), Antarctica: An Extreme Environment in a Changing World. Wiley Publishing Ltd., Berlin.

Epstein, S., Mayeda, T.K., 1953. Variation of ^{18}O content of waters from natural sources. Geochimica et Cosmochimica Acta 4, 213–224.

Fogt, R.L., Bromwich, D.H., 2006. Decadal variability of the ENSO teleconnection to the high latitude South Pacific governed by coupling with the Southern Annular Mode. Journal of Climate 19, 979–997.

Gille, S.T., 2008. Decadal-scale temperature trends in the Southern Hemisphere ocean. Journal of Climate 21, 4749–4764.

Gillett, N., Thompson, D.W.J., 2003. Simulation of recent Southern Hemisphere climate change. Science 302, 273–275.

Hofmann, E.E., Klinck, J.M., Lascara, C.M., Smith, D.A., 1996. Water mass distribution and circulation west of the Antarctic Peninsula and including Bransfield Strait. In: Ross, R.M. (Ed.), Foundations for Ecological Research West of the Antarctic Peninsula, vol. 70. American Geophysical Union, Washington DC, pp. 61–80.

Howard, S.L., Hyatt, J., Padman, L., 2004. Mixing in the pycnocline over the western Antarctic Peninsula shelf during Southern Ocean GLOBEC. Deep-Sea Research II 51, 1965–1979.

Kalnay, E., Kanamitsu, M., Kistler, R., Collins, W., Deaven, D., Gandin, L., Iredell, M., Saha, S., White, G., Woollen, J., Zhu, Y., Chelliah, M., Ebisuzaki, W., Higgins, W., Janowiak, J., Mo, K.C., Ropelewski, C., Wang, J., Leetmaa, A., Reynolds, R., Jenne, R., Joseph, D., 1996. The NCEP/NCAR 40-year reanalysis project. Bulletin of the American Meteorological Society 77, 437–471.

King, J.C., 1994. Recent climate variability in the vicinity of the Antarctic Peninsula. International Journal of Climatology 14, 357–369.

King, J.C., Harangozo, S.A., 1998. Climate change in the western Antarctic Peninsula since 1945: observations and possible causes. Annals of Glaciology 27, 571–575.

Klinck, J.M., 1998. Heat and salt changes on the continental shelf west of the Antarctic Peninsula between January 1993 and January 1994. Journal of Geophysical Research 103, 7617–7636.

Klinck, J.M., Hofmann, E.E., Beardsley, R.C., Salighoglu, B., Howard, S., 2004. Water mass properties and circulation on the West Antarctic Peninsula continental shelf in austral fall and winter 2001. Deep-Sea Research II 51, 1925–1946.

Kwok, R., Comiso, J.C., 2002. Spatial patterns of variability in Antarctic surface temperature: connections to the Southern Hemisphere Annular Mode and the Southern Oscillation. Geophysical Research Letters 29. doi:10.1029/GL015415.

Lefebvre, W., Goosse, H., 2005. Influence of the Southern Annular Mode on the sea ice-ocean system: The role of the thermal and mechanical forcing. Ocean Science 1, 145–157.
Lefebvre, W., Goosse, H., Timmermann, R., Fichefet, T., 2004. Influence of the Southern Annular Mode on the sea ice-ocean system. Journal of Geophysical Research 109.
Lehmann, M., Siegenthaler, U., 1991. Equilibrium oxygen- and hydrogen-isotope fractionation between ice and water. Journal of Glaciology 57, 23–26.
L'Heureux, M.L., Thompson, D.W.J., 2006. Observed relationships between the El-Niño/Southern Oscillation and the extratropical zonal-mean circulation. Journal of Climate 19, 276–287.
Liu, J., Curry, J.A., Martinson, D.G., 2004. Interpretation of recent Antarctic sea ice variability. Geophysical Research Letters 31.
Marshall, G.J., 2003. Trends in the Southern Annular Mode from observations and reanalyses. Journal of Climate 16, 4134–4143.
Marshall, G.J., Harangozo, S.A., 2000. An appraisal of NCEP/NCAR reanalysis MSLP data viability for climate studies in the South Pacific. Geophysical Research Letters 27, 3057–3060.
Marshall, G.J., King, J.C., 1998. Southern Hemisphere circulation anomalies associated with extreme Antarctic Peninsula winter temperatures. Geophysical Research Letters 25, 2437–2440.
Martinson, D.G., 1990. Evolution of the Southern Ocean winter mixed layer and sea ice: open ocean deepwater formation and ventilation. Journal of Geophysical Research 95, 11641–11654.
Martinson, D.G., Stammerjohn, S.E., Iannuzzi, R.A., Smith, R.C., Vernet, M., 2008. Western Antarctic Peninsula physical oceanography and spatio-temporal variability. Deep-Sea Research II 55, 1964–1987.
Massom, R.A., Stammerjohn, S.E., Lefebvre, W., Harangozo, S.A., Adams, N., Scambos, T., Pook, M.J., Fowler, C., 2008. West Antarctic Peninsula sea ice in 2005: extreme compaction and ice edge retreat due to strong anomaly with respect to climate. Journal of Geophysical Research 113.
Meredith, M.P., King, J.C., 2005. Rapid climate change in the ocean to the west of the Antarctic Penisula during the second half of the twentieth century. Geophysical Research Letters 32. doi:10.1029/2005GL024042.
Meredith, M.P., Renfrew, I.A., Clarke, A., King, J.C., Brandon, M.A., 2004. Impact of the 1997/98 ENSO on the upper waters of Marguerite Bay, western Antarctic Peninsula. Journal of Geophysical Research 109. doi:10.1029/2003JC001784.
Meredith, M., Brandon, M.A., Wallace, M.I., Clarke, A., Leng, M.J., Renfrew, I.A., van Lipzig, N.P.M., & King, J.C., 2008a. Variability in the freshwater balance of northern Marguerite Bay, Antarctic Peninsula: results from δ^{18}O Deep-Sea Research II, 55, 309–322.
Meredith, M.P., Murphy, E.J., Hawker, E.J., King, J.C., Wallace, M.I., 2008b. On the interannual variability of ocean temperatures around South Georgia, Southern Ocean: forcing by El Niño/Southern Oscillation and the Southern Annular Mode. Deep-Sea Research II 55, 2007–2022.
Mitchell, B.G., Holm-Hansen, O., 1991. Observations and modeling of the Antarctic phytoplankton crop in relation to mixing depth. Deep-Sea Research 38, 981–1007.
Moffat, C., Beardsley, R., Owens, W.B., van Lipzig, N., 2008. A first description of the Antarctic Peninsula Coastal Current. Deep-Sea Research II 55, 277–293.
Moffat, C., Owens, B., Beardsley, R.C., 2009. On the characteristics of circumpolar deep water intrusions to the west Antarctic Peninsula continental shelf. Journal of Geophysical Research 114, C05017.
Montes-Hugo, M., Doney, S.C., Ducklow, H.W., Fraser, W., Martinson, D., Stammerjohn, S.E., Schofield, O., 2009. Recent changes in phytoplankton communities associated with rapid regional climate change along the western Antarctic Peninsula. Science 323, 1470–1473.
Mosby, H., 1934. The waters of the Atlantic Antarctic Ocean. Scientific Results of the Norwegian Antarctic Expedition 1927–1928 (11), 1–131.
Östlund, H.G., Hut, G., 1984. Arctic Ocean water mass balance from isotope data. Journal of Geophysical Research 89, 6373–6381.
Potter, J.R., & Paren, J.G., 1985. Interaction Between Ice Shelf and Ocean in George VI Sound, Antarctica. Oceanology of the Antarctic Continental Shelf, American Geophysical Union, 43, 35–58.
Price, J.F., Weller, R.A., Pinkel, R., 1986. Diurnal cycling: observations and models of the upper ocean response to diurnal heating, cooling and wind mixing. Journal of Geophysical Research 91.
Renfrew, I.A., King, J.C., Markus, T., 2002a. Coastal polynyas in the southern Weddell Sea: variability of the surface energy budget. Journal of Geophysical Research 107. doi:10.10129/12000JC000720.
Renfrew, I.A., Moore, G.W.K., Guest, P.S., Bumke, K., 2002b. A comparison of surface-layer and surface turbulent-flux observations over the Labrador Sea with ECMWF analyses and NCEP reanalyses. Journal of Physical Oceanography 32, 383–400.
Savidge, D.K., Amft, J.A., 2009. Circulation on the West Antarctic Peninsula derived from 6 years of ADCP transects. Deep-Sea Research I 56, 1633–1655.
Schlosser, P., Bayer, R., Foldvik, A., Gammelsrod, T., Rohardt, G., Munnich, K.O., 1990. Oxygen 18 and helium as tracers of Ice Shelf Water and water/ice interaction in the Weddell Sea. Journal of Geophysical Research 95, 3253–3263.
Schlosser, P., Newton, R., Ekwurzel, B., Khatiwala, S., Mortlock, R., Fairbanks, R., 2002. Decrease of river runoff in the upper waters of the Eurasian Basin, Arctic Ocean, between 1991 and 1996: evidence from δ^{18}O data. Geophysical Research Letters 29. doi:10.1029/2001GL013135.
Schofield, O., Ducklow, H.W., Martinson, D.G., Meredith, M.P., Moline, M.A., Fraser, W.R., 2010. How do polar marine ecosystems respond to rapid climate change? Science 328, 1520.
Smith, S.D., 1988. Coefficients for sea surface wind stress, heat flux, and wind profiles as a function of wind speed and temperature. Journal of Geophysical Research 93, 15467–15472.
Smith, D.A., Klinck, J.M., 2002. Water properties on the west Antarctic Peninsula continental shelf: a model study of effects of surface fluxes and sea ice. Deep-Sea Research II 49, 4863–4886.
Smith, R.C., Stammerjohn, S.E., 2001. Variations of surface air temperature and sea ice extent in the western Antarctic Peninsula (WAP) region. Annals of Glaciology 33, 493–500.
Smith, D.A., Hofmann, E.E., Klinck, J.M., Lascara, C.M., 1999. Hydrography and circulation of the West Antarctic Peninsula continental shelf. Deep-Sea Research I 46, 925–949.
Stammer, D., Wunsch, C., Ueyoshi, K., 2006. Temporal changes in ocean eddy transports. Journal of Physical Oceanography 36, 543–550.
Stammerjohn, S.E., Martinson, D.G., Smith, R.C., Ianuzzi, R.A., 2008a. Sea ice in the western Antarctic Peninsula region: spatio-temporal variability from ecological and climate change perspectives. Deep-Sea Research II 55.
Stammerjohn, S.E., Martinson, D.G., Smith, R.C., Yuan, X., Rind, D., 2008b. Trends in Antarctic annual sea ice retreat and advance and their relation to El Niño-Southern Oscillation and Southern Annular Mode variability. Journal of Geophysical Research 113.
Steig, E.J., Schneider, D.P., Rutherford, S.D., Mann, M.E., Comiso, J.C., Shindell, D.T., 2009. Warming of the Antarctic ice-sheet surface since the 1957 International Geophysical Year. Nature 457, 459–462.
Stein, M., 1992. Variability of local upwelling off the Antarctic Peninsula, 1986–1990. Archiv Fischereiwissenschaft 41, 131–158.
Thoma, M., Jenkins, A., Holland, D., Jacobs, S., 2008. Modelling circumpolar deep water intrusions on the Amundsen Sea continental shelf, Antarctica. Geophysical Research Letters 35, L18602.
Thomas, E.R., Marshall, G.J., McConnell, J.R., 2008. A doubling in snow accumulation in the Western Antarctic Peninsula. Geophysical Research Letters 35.
Thomas, E.R., Dennis, P.F., Bracegirdle, T.J., Franzke, C., 2009. Ice core evidence for significant 100-year regional warming on the Antarctic Peninsula. Geophysical Research Letters 36.
Thompson, D.W.J., Solomon, S., 2002. Interpretation of recent Southern Hemisphere climate change. Science 296, 895–899.
Thompson, D.W.J., Wallace, J.M., 2000. Annular modes in the extratropical circulation. Part I: month-to-month variability. Journal of Climate 13, 1000–1016.
Thompson, D.W.J., Wallace, J.M., Hegerl, G.C., 2000. Annular modes in the extratropical circulation. Part II: trends. Journal of Climate 13, 1018–1036.
Trenberth, K.E., Jones, P.D., Ambenje, P., Bojariu, R., Easterling, D., Tank, A.K., Parker, D., Rahimzadeh, F., Renwick, J.A., Rusticucci, M., Soden, B., Zhai, P., 2007. Observations: surface and atmospheric climate change. In: Solomon, D.Q.S., Manning, M., Chen, Z., Marquis, M., Averyt, K.B., Tignor, M., Miller, H.L. (Eds.), Climate Change 2007: The Physical Science Basis. Contributions of Working Group 1 to the Fourth Assessment Report of the Intergovernmental Panel on Climate Change. Cambridge University Press, Cambridge.
Turner, J., 2004. The El Niño-Southern Oscillation and Antarctica. International Journal of Climatology 24, 1–31.
Turner, J., Colwell, S.R., Harangozo, S., 1997. Variability of precipitation over the coastal western Antarctic Peninsula from synoptic observations. Journal of Geophysical Research 102, 13999–14007.
Turner, J., Colwell, S.R., Marshall, G.J., Lachlan-Cope, T.A., Carleton, A.M., Jones, P.D., Lagun, V., Reid, P.A., Iagovinka, S., 2005. Antarctic climate change during the last 50 years. International Journal of Climatology 25, 279–294.
Turner, J., Comiso, J.C., Marshall, G.J., Lachlan-Cope, T.A., Bracegirdle, T., Maksym, T., Meredith, M.P., Wang, Z., Orr, A., 2009. Non-annular atmospheric circulation change induced by stratospheric ozone depletion and its role in the recent increase in Antarctic sea ice extent. Geophysical Research Letters 36, L08502.
Vaughan, D.G., 2006. Recent trends in melting conditions on the Antarctic Peninsula and their implications for ice-sheet mass balance and sea level. Arctic, Antarctic and Alpine Research 38, 147–152.
Vaughan, D.G., Marshall, G.J., Connolley, W.M., Parkinson, C., Mulvaney, R., Hodgson, D.A., King, J.C., Pudsey, C.J., Turner, J., 2003. Recent rapid regional climate warming on the Antarctic Peninsula. Climatic Change 60, 243–274.
Wallace, M.I., Meredith, M.P., Brandon, M.A., Sherwin, T.J., Dale, A., Clarke, A., 2008. On the characteristics of internal tides and coastal upwelling behaviour in Marguerite Bay, west Antarctic Peninsula. Deep-Sea Research II 55, 2023–2040.
Weiss, R.F., Östlund, H.G., Craig, H., 1979. Geochemical studies of the Weddell Sea. Deep-Sea Research 26A, 1093–1120.
Weppernig, R., Schlosser, P., Khatiwala, S., Fairbanks, R.G., 1996. Isotope data from Ice Station Weddell: implications for deep water formation in the Weddell Sea. Journal of Geophysical Research 101. 25, 723–725, 739.
Yuan, X., 2004. ENSO-related impacts on Antarctic Sea Ice: synthesis of phenomemon and mechanisms. Antarctic Science 16, 415–425.